

**Capture of Sulfur Dioxide using Sulfur Oxydianions: Synthesis and
Characterization of Two Novel Compounds**

by

Stephanie Richardson

Bachelor of Science – Chemistry, UNB, 2009

A Thesis Submitted in Partial Fulfillment
of the Requirements for the Degree of

Masters of Science

in the Graduate Academic Unit of Chemistry

Supervisor: Jack Passmore, PhD. Chemistry

Examining Board: Jack Passmore, PhD., Chemistry
Friedrich Grein, PhD., Chemistry, chair
Ben Newling, PhD., Physics

This thesis is accepted by the
Dean of Graduate Studies

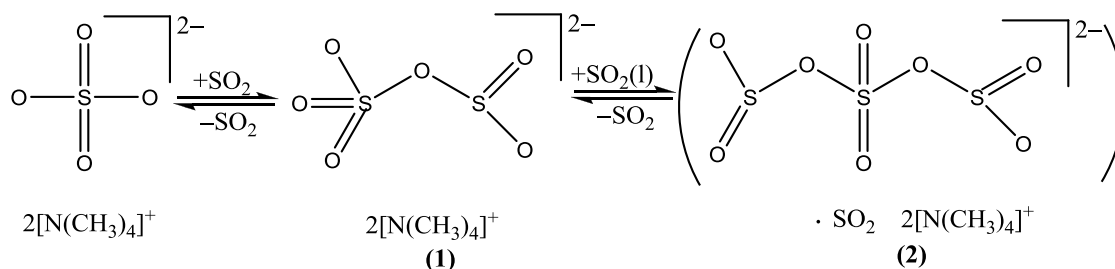
THE UNIVERSITY OF NEW BRUNSWICK

June, 2013

© Stephanie Richardson 2013

ABSTRACT

One mole equivalent of SO_2 reversibly reacts with $[\text{N}(\text{CH}_3)_4]_2\text{SO}_4(\text{s})$ to give $[\text{N}(\text{CH}_3)_4]_2\text{S}_2\text{O}_6(\text{s})$ (**1**) containing the $[\text{O}_3\text{SOSO}_2]^{2-}$ ion, shown by Raman and IR to be an isomer of the $[\text{O}_3\text{SSO}_3]^{2-}$ dianion. The experimental and calculated (B3PW91/6-311+G(3df)) vibrational spectra are in excellent agreement and the IR spectrum is similar to that of the isoelectronic $\text{O}_3\text{ClOClO}_2$. Crystals of $[\text{N}(\text{CH}_3)_4]_2(\text{O}_2\text{SO})_2\text{SO}_2 \cdot \text{SO}_2$ were isolated from a solution of $[\text{N}(\text{CH}_3)_4]_2\text{SO}_4$ in liquid SO_2 . The X-ray structure showed that it contained the $[(\text{O}_2\text{SO})_2\text{SO}_2]^{2-}$ dianion (**2**). The characterized $\text{N}(\text{CH}_3)_4^+$ salts **1** and **2** are the first two members of the $(\text{SO}_4)(\text{SO}_2)_x^{2-}$ sulfur oxydianions analogous to the well-known small cation salts of the $\text{SO}_4(\text{SO}_3)_x^{2-}$ polysulfates.



DEDICATION

This thesis is dedicated to my mother (Dixie), grandmother (Annie) and uncle (Terry).

ACKNOWLEDGEMENTS

First, I would like to thank my supervisor Jack Passmore for all the patience and encouragement he has given me through this journey. My co-supervisor, Sean McGrady, has been an inspiration in my chemistry career. I am very grateful for being part of an amazing group through the last few years. Scott Greer has encouraged me and has been my mentor. The four post docs, Tressia Paulose, Mikko Rautiainen, Arun Kumar and Birgit Muller have given me guidance when I was in the dark and have taught me a lot of theory and laboratory chemistry. Sandra Riley is a wonderful chemical technician and has been able to show me as well as teach me about the equipment needed to characterize compounds. Sarah Ackermann and many new other friends have been a delight to be around. Dr. Fritz Grein and Pablo Bruna have been exceptional at producing theoretical results for my project as well as helping me understand computational chemistry.

The staff members at UNB always have a smile on their face and have helped me during my degree. A big thank you to Krista Coy, Ed Goodfellow, Brian Malcolm, Adam Fowler, David Green and Gilles Vautour.

Lastly and arguably most important would be my family. My mother, Dixie Richardson, is a person I can always count on and has listened to my problems as well as my successes throughout my masters. My grandmother, Annie Richardson, is my role model and I can only hope to blossom into a hard working woman like herself. My uncle, Terry Richardson, is an important male role model in my life even though he is a Toronto Maple Leafs fan.

All in all, I have been blessed to be around and work with so many wonderful people and can only hope that I will be as lucky in my future career.

Table of Contents

DEDICATION	iii
ABSTRACT	ii
ACKNOWLEDGEMENTS	iv
Table of Contents	v
List of Tables	vi
List of Figures	viii
List of Symbols, Nomenclature or Abbreviations	xii
Chapter 1. Introduction	1
Chapter 2. The Synthesis of $[\text{N}(\text{CH}_3)_4]_2\text{O}_3\text{SOSO}_2(\text{s})$ and $[\text{N}(\text{CH}_3)_4]_2[(\text{O}_2\text{SO})_2\text{SO}_2]\cdot\text{SO}_2(\text{s})$ Containing $(\text{SO}_4)(\text{SO}_2)_x^{2-}$ $x = 1, 2$, Members of a New Class of Sulfur Oxydianions	19
Chapter 3. Conclusions and Future Work	47
Supporting Information	53
Curriculum Vitae	

List of Tables

Table 1.1. Known Sulfur Oxydianions Containing 1 - 3 Sulfur Atoms in the Solid State.	11
Table 2.2. The experimental vibrational spectrum (frequencies cm^{-1} , relative intensities in brackets) of $[\text{O}_3\text{SOSO}_2]^{2-}$ in $[\text{N}(\text{CH}_3)_4]_2\text{O}_3\text{SOSO}_2(\text{s})$, compared with the calculated (B3PW91/6-311+G(3df)) spectrum and the isoelectronic $\text{O}_3\text{ClOClO}_2(\text{g})$	33
Table 2.3. The experimental vibrational spectrum (frequencies cm^{-1} , relative intensities in brackets) attributed to $[(\text{O}_2\text{SO})_2\text{SO}_2]^{2-}$ in the solid obtained from the addition of 2.07 mole equivalent of SO_2 to 1 mole of $[\text{N}(\text{CH}_3)_4]_2\text{SO}_4(\text{s})$, compared with the calculated (B3PW91/6-311+G(3df)) spectrum of $[(\text{O}_2\text{SO})_2\text{SO}_2]^{2-}$	39
Table 3.1. New and Known Sulfur Oxydianions Containing 1 - 5 Sulfur Atoms in the Solid State.	49
Table S.1. Estimation of the Gibbs free energy (298 K) for the uptake of $\text{SO}_2(\text{g})$ by $\text{R}_2\text{SO}_4(\text{s})$	55
Table S.2. The experimental vibrational spectrum (frequencies cm^{-1} , relative intensities in brackets) of $[\text{O}_3\text{SOSO}_2]^{2-}$ in $[\text{N}(\text{CH}_3)_4]_2\text{O}_3\text{SOSO}_2(\text{s})$, compared with the calculated (B3PW91/6-311+G(3df)) spectrum.	63
Table S.3. Comparison of Cl_2O_6 , the calculated $[\text{O}_3\text{SOSO}_2]^{2-}$ and peaks attributed to $[\text{O}_3\text{SOSO}_2]^{2-}$ in $[\text{N}(\text{CH}_3)_4]_2\text{O}_3\text{SOSO}_2(\text{s})$, with frequencies cm^{-1} and relative intensities in brackets.	65
Table S.4. Crystal data and structure refinement for $[\text{N}(\text{CH}_3)_4]_2(\text{O}_2\text{SO})_2\text{SO}_2 \cdot \text{SO}_2(\text{s})$	70

Table S.5. The experimental vibrational spectrum (frequencies cm^{-1} , relative intensities in brackets) of $[(\text{O}_2\text{SO})_2\text{SO}_2]^{2-}$ in the solid obtained from the addition of 2.07 mole equivalent of SO_2 to 1 mole of $[\text{N}(\text{CH}_3)_4]_2\text{SO}_4(\text{s})$, compared with the calculated (B3PW91/6-311+G(3df)) spectrum.....	72
Table S.6. A comparison of Av S-O bond distances (\AA), OSO bond angle ($^\circ$) and Raman frequency (frequencies cm^{-1} , relative intensities in brackets) in $[\text{N}(\text{CH}_3)_4]_2\text{O}_3\text{SOSO}_2 \cdot \text{SO}_2(\text{s})$, $\text{SO}_2(\text{g})$ and $\text{SO}_2(\text{s})$	75
Table S.7. Cation anion contacts in $[\text{N}(\text{CH}_3)_4]_2(\text{O}_2\text{SO})_2\text{SO}_2 \cdot \text{SO}_2(\text{s})$	78
Table S.8. Comparison of the geometry of $[\text{N}(\text{CH}_3)_4]^+$ in $[\text{N}(\text{CH}_3)_4]_2(\text{O}_2\text{SO})_2\text{SO}_2 \cdot \text{SO}_2$ to other known $[\text{N}(\text{CH}_3)_4]^+$ salts.	78

List of Figures

Figure 1.1. Resonance Structures of SO ₂	7
Figure 1.2. SO ₂ molecular orbital model of the π system. Net π bond order for A = 0 and B = 1.....	8
Figure 1.3. Valence Bond Description of the Bonding in Sulfate.	12
Figure 2.1. Born-Haber cycle for reaction of R ₂ SO ₄ (s) + SO ₂ (g) where R = N(CH ₃) ₄ ⁺ (blue) and Na ⁺ (red).	21
Figure 2.2. Estimated ΔG_{rxn} (298 K) for equation 2.4 and 2.5 as shown below:.....	22
Figure 2.3. The Raman spectrum of [N(CH ₃) ₄] ₂ [O ₃ SOSO ₂](s) (B) compared with the calculated (B3PW91/6-311+G(3df)) Raman spectrum of [O ₃ SOSO ₂] ²⁻ (g) (A) in the 140 - 1500 cm ⁻¹ region. Scans: 2048; resolution: 4cm ⁻¹ ; laser power: 0.205 W; Ge detector. Spectra of the 1500-3500 cm ⁻¹ region included in Figure S.2. Assignments related to N(CH ₃) ₄ ⁺ and SO ₄ ²⁻ were made by comparison with those in [N(CH ₃) ₄] ₂ SO ₄ (s) and SO ₂ of solvation with similar compounds found in Table S.6.	32
Figure 2.4. Calculated (B3PW91/6-311+G(3df)) structure of [O ₃ SOSO ₂] ²⁻ in the gas phase; bond lengths (Å) (red), [bond orders] (black) and Mulliken charges (blue). <O2-S1-O1: 113.06, <O1-S1-O3: 113.06, <O3-S1-O4: 107.29, <O4-S1-O2: 107.29, <S1-O4-S2: 121.88, <O4-S2-O6: 100.26, <O6-S2-O5: 111.40, <O5-S2-O4: 100.26.	34
Figure 2.5. A comparison of calculated (B3PW91/6-311+G(3df)) bond lengths, bond angles, bond order and charge in SO ₂ (A), SO ₄ ²⁻ (B) and HOSO ₂ ²⁻ (C); bond lengths (Å) (red), bond orders (black), bond angles (green) and Mulliken charges (blue). *Experimental bond lengths and angles for SO ₄ ²⁻ in [N(CH ₃) ₄] ₂ SO ₄ (s), S-O (Å):	

1.461(2), <OSO (°): 109.51(9), 109.4(2) and SO ₂ (s), S-O (Å):1.4297(7), <OSO (°): 117.5(1)). Calculated (B3LYP/6-31G(2df,p)) bond lengths of [O ₂ SOH] ⁻²² , S-O (Å): 1.494, 1.482, 1.768, O-H (Å): 96.6.....	35
Figure 2.6. A valence bond description of [O ₃ SOSO ₂] ²⁻	35
Figure 2.7. [A] Diamond depiction of [(O ₂ SO) ₂ SO ₂] ²⁻ in [N(CH ₃) ₄] ₂ (O ₂ SO) ₂ SO ₂ •SO ₂ (s) (thermal ellipsoid plots are at the 50% probability level). Bond length (Å) (black) and bond angles (°) (blue). [B] Calculated structure of [(O ₂ SO) ₂ SO ₂] ²⁻ in gas phase; bond lengths (Å) (grey), bond orders (black), and Mulliken charges (blue). Select bond angles (°): <O5-S2-O6: 113.1 <O6-S2-O1: 101.1, <O1-S2-O5: 97.8, S2-O1-S1: 122.6, <O1-S1-O3: 109.7, <O3-S1-O4: 115.9, <O4-S1-O2: 109.7, <O2-S1-O1: 105.7, <S1-O2-S3: 122.6, <O2-S3-O8: 101.1, <O8-S3-O7: 113.1, <O7-S3-O2: 97.8.	37
Figure 2.8. Calculated (B3PW91/6-31+G*) structure of (O ₂ SO) ₂ (SO ₂) ₂ ²⁻	37
Figure 2.9. A portion of the layer of [(O ₂ SO) ₂ SO ₂] ²⁻ anion and weakly interacting SO ₂ molecules of solvation in ab plane, bond distances (Å) and [bond orders] (thermal ellipsoid plots are drawn at the 50% probability level).	40
Figure 2.10. Valence bond description of [(O ₂ SO) ₂ SO ₂] ²⁻	42
Figure S.1. Illustration of vessels A and B.	57
Figure S.2. Raman spectra of [N(CH ₃) ₄] ₂ O ₃ SOSO ₂ (A) and [N(CH ₃) ₄] ₂ SO ₄ + 2SO ₂ (B) in 140 - 4000 cm ⁻¹ region (Scans: 2048; Resolution: 4cm ⁻¹ ; Detector: Ge) with 0.205 power.....	59
Figure S.3. Raman spectra of a 1:1 SO ₂ :[N(CH ₃) ₄] ₂ SO ₄ (s) as a function of time in the 140 - 1500 cm ⁻¹ region compared with the calculated spectrum, D of [O ₃ SOSO ₂] ²⁻ . Scans:	

2048; resolution: 4cm^{-1} ; laser power: 0.205 W where (A) (C) use Ge detector and (B) use InGaAs detector . Spectra of the $1500\text{-}3500\text{ cm}^{-1}$ region after 7 days included in Figure S.2. Assignments related to $\text{N}(\text{CH}_3)_4^+$ and SO_4^{2-} were made by comparison with those in $[\text{N}(\text{CH}_3)_4]_2\text{SO}_4(\text{s})^7$ and SO_2 of solvation with similar compounds found in Table S.6. 60

Figure S.4. Infrared spectra of $[\text{N}(\text{CH}_3)_4]_2\text{O}_3\text{SOSO}_2(\text{s})$ (scans: 32; Resolution: 4cm^{-1}) compared with starting material, $[\text{N}(\text{CH}_3)_4]_2\text{SO}_4(\text{s})$, and calculated spectra of $[\text{O}_3\text{SOSO}_2]^{2-}$ in $140 - 1400\text{ cm}^{-1}$ region. Spectra of the $1500\text{-}3500\text{ cm}^{-1}$ region is given in S.5. Assignments related to $\text{N}(\text{CH}_3)_4^+$ and SO_4^{2-} were made by comparison with those in $[\text{N}(\text{CH}_3)_4]_2\text{SO}_4(\text{s})$.⁷ There are also bands that are attributed to SO_4^{2-} that likely come from the loss of SO_2 from the $[\text{O}_3\text{SOSO}_2]^{2-}$ on sample preparation. 61

Figure S.5. Infrared spectra of $[\text{N}(\text{CH}_3)_4]_2\text{O}_3\text{SOSO}_2$ compared with that of the starting material, $[\text{N}(\text{CH}_3)_4]_2\text{SO}_4$, in $140 - 4000\text{ cm}^{-1}$ region (scans: 32; Resolution: 4cm^{-1}). 62

Figure S.6. Calculated (B3PW91/6-311+G(3df)) gas phase structure of $[\text{O}_3\text{SOSO}_2]^{2-}$ with bond lengths (\AA). 67

Figure S.7. Calculated (B3PW91/6-311+G(3df)) gas phase structure of Cl_2O_6 with bond lengths (\AA). 67

Figure S.8. Loss of SO_2 on evacuation of $[\text{N}(\text{CH}_3)_4]_2\text{O}_3\text{SOSO}_2(\text{s})$ as a function of time. 68

Figure S.9. Raman of $[\text{N}(\text{CH}_3)_4]_2\text{SO}_4(\text{s})$ after the removal of SO_2 (B) from $[\text{N}(\text{CH}_3)_4]_2\text{O}_3\text{SOSO}_2(\text{s})$ (A) compared with that of $[\text{N}(\text{CH}_3)_4]_2\text{SO}_4(\text{s})$ (C) in $140 - 1500\text{ cm}^{-1}$ region (Scans: 2048; Resolution: 4cm^{-1} ; Detector: Ge) with A and B laser power of 0.205 W and C laser power of 0.216 W..... 69

Figure S.10. Raman of $[\text{N}(\text{CH}_3)_4]_2\text{SO}_4 + 2.07 \text{SO}_2(\text{s})$ obtained after 5 days (C) compared with that of $[\text{N}(\text{CH}_3)_4]\text{SO}_4(\text{s})$ (D) and calculated spectrum of $[(\text{O}_2\text{SO})_2\text{SO}_2]^{2-}$ (A) in 160 - 1300 cm^{-1} region (resolution: 4cm^{-1}) where (C) has 1024 scans, use InGaAs detector and laser power of 0.205 W and (D) has 2048 scans, use Ge detector and laser power of 0.216 W. (A) and (B) are calculated spectra.....	71
Figure S.11. TGA of $[\text{N}(\text{CH}_3)_4]_2\text{O}_3\text{SOSO}_2$. Blue numbers indicated expected weight percent and red numbers indicate experimental value.....	74
Figure S.12. DSC of $[\text{N}(\text{CH}_3)_4]_2\text{O}_3\text{SOSO}_2$. TGA outlined in grey.....	74
Figure S.13. TGA of $[\text{N}(\text{CH}_3)_4]_2\text{O}_3\text{SOSO}_2$ as a function of time.....	75
Figure S.14. Frequency of S-O bond distances from Cambridge Crystallographic Data Centre (August 2011).....	76
Figure S.15. Diamond depiction of $\text{N}(\text{CH}_3)_4^+$ in $[\text{N}(\text{CH}_3)_4]_2(\text{O}_2\text{SO})_2\text{SO}_2 \cdot \text{SO}_2(\text{s})$	77
Figure S.16. Crystal packing of $[\text{N}(\text{CH}_3)_4]_2(\text{O}_2\text{SO})_2\text{SO}_2 \cdot \text{SO}_2(\text{s})$ along the a axis using 2 x 2 x 2 unit cells. Hydrogen atoms were removed for clarity.....	77

List of Symbols, Nomenclature or Abbreviations

Å – Angstroms

R.T. – Room temperature

VSEPR – Valence shell electron pair repulsion

cm^{-1} – reciprocal centimeter (wavenumber)

T – Temperature

C – Celcius

SO₂ – sulfur dioxide

(s) - solid

(g) - gas

(l) - liquid

δ - bending

ν - stretching

H – Enthalpy

G – Gibbs free Energy

S - Entropy

Δ - change of a variable

a.u – atomic units

rxn – reaction

mol - mole

kJ – kilojoules

K - kelvin

IR – infrared

nm³ – nanometer cubed

DFT – density functional theory

R – gas constant

Ge detector – germanium detector

Int – intensity

%T - % transmittance

V.B.T – volume based thermodynamics

z – charge on ion

Chapter 1. Introduction

1.A. SO₂ the Pollutant, the Problem and Some Current Solutions.

1.1.A. SO₂ the Pollutant.

Sulfur dioxide is an air pollutant that arises from both natural sources and human activity.¹ SO₂ in the atmosphere reacts with oxygen in the presence of UV light at high altitudes to form SO₃; SO₃ then reacts with water vapour to produce sulfuric acid, a component of acid rain as shown in reactions **1.1** and **1.2**.^{2,3}



Acid rain changes the pH of lakes and as a consequence harms plant life and aquatic life and also erodes away some buildings (e.g. limestone construction) as seen in equations **1.3** and **1.4**.¹



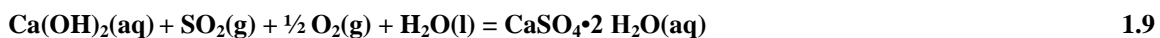
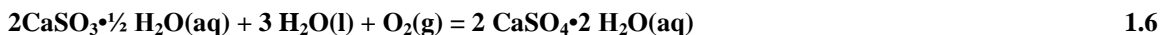
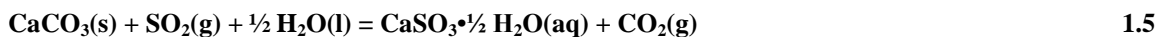
Sulfur dioxide is toxic and exposure can cause severe health problems, it is important to control emissions of this pollutant. Sulfur dioxide is released naturally (volcanoes, biological reduction of sulfur compounds and in sea-spray)² but the quantities are normally minimal compared to the SO₂ released into the atmosphere by industries. Anthropogenic SO₂ is produced primarily through the burning of fossil fuels (coal, fuel oil, natural gas) and from the smelting of non-ferrous metals.¹ Worldwide, emissions of anthropogenic SO₂ are expected to increase by 50% by the end of 2020.¹ Sudbury,

Ontario, a major center for smelting operations, is one of the largest SO₂ emitters in the world; in the time period 1885 – 1929 emitters in Sudbury released more than 100 million tons of SO₂ into the atmosphere.⁴ In 1960, SO₂ emissions from smelting operations in Sudbury were at their peak and Sudbury was responsible for approximately 4% of global sulfur emissions.⁴ While the amount of SO₂ released in Sudbury has decreased over the past 50 years, in 1995 emitters there were given a regulatory limit of 365,000 tonnes of SO₂/year. At this time, non-ferrous metal smelting in Sudbury remains one of the largest sources of SO₂ emissions world wide.⁴

The continued release of anthropogenic SO₂ into the atmosphere on very large scales and the damaging nature of SO₂ air pollution make the search for more effective means of capturing SO₂ very relevant to modern industrial chemistry. Therefore, one of the main foci of this research was to discover a compound that would absorb and release SO₂ under mild conditions and to characterize the absorption product.

1.1.B. Present Industrial SO₂ Capture Processes.

In industry, the SO₂ that is produced by burning fossil fuels is captured but it is an expensive procedure that is not efficient.¹ The processes to remove SO₂ after the fossil fuels have been burned in industry have been reviewed by Pandey, Biswas, Chakrabarti and Devotta and have been categorized into non regenerative and regenerative processes that include wet scrubbing and dry scrubbing.¹ Industries need the process to be cost effective and preferably re-generable. Today, the more common processes used in industry to remove SO₂ are called the wet limestone process (wet scrubbing), shown in equations **1.5** and **1.6** and wet lime scrubbing (wet scrubbing), shown in equations **1.7 - 1.9**.^{1,5}



The main problem with these processes is that the calcium sulfate (gypsum) produced is a waste product and it also builds up in the equipment.¹ Some of the other processes overcome this problem but contribute to new problems. Industrial process can re-generate the SO₂ but the material needs to be heated to high temperatures and this represents a major operating expense. To date, there is not a compound that can recycle SO₂ cost effectively in an industrial setting.

Over the last 50 to 100 years, scientists have agreed that SO₂ and other gases are a serious environmental problem and have begun focusing on this environmental crisis by trying to find compounds that will efficiently absorb and release pollutant gases such as CO₂ and SO₂.⁶

1.1.C. Research-Stage SO₂ Capture Strategies.

Finding a method to remove the SO₂ at the industrial level begins in the laboratory. Some well-studied compounds that react with SO₂ producing charge transfer complexes are triethylamine (ie [N(CH₃)₃•SO₂]) and salts of halides (ie [N(CH₃)₄]Cl•SO₂).^{7,8,9,10} Both complexes are known as charge transfer compounds. Lippincott observed in Raman and Infrared spectroscopy a shift in the ν_s S-O in simple halide salts and concluded that the shift of the ν_s S-O was due to the formation of a charge transfer complex.¹⁰ He concluded that the larger the shift from the known 1150 cm⁻¹ for

the ν_s S-O in free SO₂ the stronger the charge transfer.¹⁰ The SO₂ band in the vibrational spectra of two novel compounds is presented in Chapter 2.

Sulfur dioxide can also be absorbed by some ionic liquids. Ionic liquids are salts with melting points below 100 °C.⁵ Some ionic liquids (eg. 1-*n*-hexyl-3-methylimidazolium bis(trifluoromethylsulfonyl)imide ([hmim][Tf₂N])¹¹, 1-*n*-hexyl-3-methylpyridinium bis(trifluoromethylsulfonyl)imide ([hmpy][Tf₂N])¹², 1-*n*-butyl-3-methylimidazolium acetate ([bmim][Ac])¹¹ and 1-*n*-butyl-3-methylimidazolium methyl sulfate ([bmim][MeSO₄])¹¹ have been investigated for the absorption of SO₂ as well as other flue gases. The absorption of SO₂ using ionic liquids is a new area. An advantage of this process is that flue gases contain several different gases and some ionic liquids are able to capture and separate them individually.¹¹ Some other advantages include the high absorption capacity of the gas at room temperature that are reversible without any change to the compounds. IL's have low vapour pressure and high thermal and chemical stability.¹³ A main disadvantage for IL's is that they have a high viscosity and therefore higher operating costs of circulating the IL.¹⁴

Another newer development in the absorption of SO₂ utilizes metal-organic frameworks (MOFs). Metal-organic frameworks are crystalline porous materials, the structures of which are composed of metal-oxide units joined by organic linkers through strong covalent bonds.¹⁵ Some MOFs that adsorb SO₂ include 1D Zn₂O₂(CO₂)₂ chains linked by 2,5-dihydroxyterephthalate, Cu₂(CO₂)₄ cluster linked by trimesate and BPL carbon.¹⁵ An advantage of using MOF's compared to other methods are that they have high effective surface areas and high thermal stability.¹⁵ A main disadvantage for MOFs

is capturing gases that are in mixtures or contain impurities which may interfere with the capture process.¹⁵

The accidental uptake of SO₂ by salts of sulfur oxydianions has been reported. Elschenbroich and colleagues accidentally obtained a very small amount of crystals of a double SO₂ solvate coordinating to the known [O₃SSO₃]²⁻; the counter cation was (η⁶-C₆H₆)₂Cr⁺.¹⁶ The [O₃SSO₃]²⁻ anion is the isomer of the [O₃SOSO₂]²⁻ anion prepared and characterized in this work. The new anion was prepared by the purposeful reversible quantitative absorption of SO₂ using SO₄²⁻ in N(CH₃)₄SO₄(s) which is presented in Chapter 2.

1.B. Properties of Sulfur Dioxide.

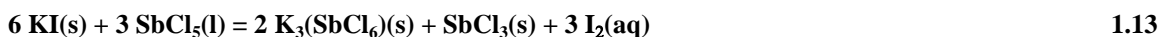
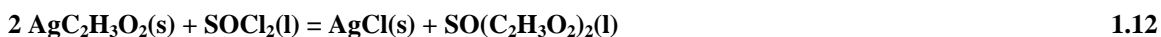
1.2.A. Physical Properties.

Sulfur dioxide is a gas under standard conditions. It has a melting point of -75.5 °C and a boiling point of -10 °C, a dipole moment of 1.62 D and a dielectric constant of 15.4 (0 °C).² The vapour pressure of SO₂ at R.T. is 3.34 atm.¹⁷ SO₂ is stored and transported as a liquid under pressure in steel cylinders and is readily handled in a closed system vacuum line (see Chapter 2).

1.2.B. SO₂ as a Solvent.

Sulfur dioxide is readily available, is non-corrosive, has a low reactivity (contains no protons), is nonflammable and is anhydrous making it a good solvent.^{18,19} Ionic compounds dissolve in SO₂ when the solvation energy is higher than the lattice energy and many covalent compounds are also soluble in SO₂.¹⁸ Sulfur dioxide is readily used in Friedel-Crafts reactions, esterification of phenols, sulfonation, sulfation, addition of

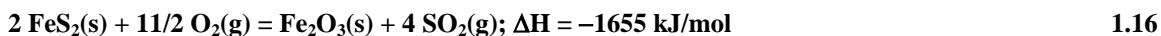
bromine to olefins, preparation of anhydrous hydrogen bromide and addition of hydrogen bromide to olefins.¹⁹ Sulfur dioxide can form solvates (Eq. **1.10**) and undergo solvolysis (Eq. **1.11**) but is a good solvent for some metathesis reactions (Eq. **1.12**), oxidation-reduction reactions (Eq. **1.13**) and complex compound formation (Eq. **1.14**).²⁰



SO₂ has also been used as a solvent in electrochemical processes (ie Cu(III) generated and stabilized by Cu(pyO)₄²⁺ (pyO= pyridine N-oxide)).²¹ The work presented in Chapter 2 shows SO₂ acting as a reactive solvent.

1.2.C. Preparation of SO₂ in the Laboratory and Commercially.

Currently, sulfur dioxide is prepared commercially by the combustion of sulfur in air (Eq. **1.15**) or by passing hot air over sulfide ores (Eq. **1.16**).²



In the laboratory, sulfur dioxide can be prepared by the reaction of copper and concentrated sulfuric acid on heating (Eq. **1.17**).²²



1.2.D. Structure/Bonding of SO₂.

Understanding reactions of SO₂ (e.g. sulfur dioxide and water in the presence of UV light) requires an understanding of the structure and bonding in the reactants. The bonding in SO₂ has been debated in the literature for many years.²³ The simplest view of sulfur dioxide obeys the octet rule and is represented in Figure 1.1 **B** and **B'**. Experimentally SO₂(g) has been shown to be a bent molecule and this can be accounted for by VSEPR.²⁴ Structure determination of SO₂(g) using electron diffraction found equal S-O bond lengths of 1.4343(3) Å (B.O: 1.85)ⁱ and a bond angle of 119.5(10) degrees.²⁴ The shorter bond length when compared to an S-O single bond (1.70 Å)ⁱ suggest that there may be double bonds involved in the structure as is represented in Figure 1.1 **A** involving a hypervalent sulfur atom. The valence bond approach accounts for the structure by 3 main resonance structures of SO₂ as shown below²³:

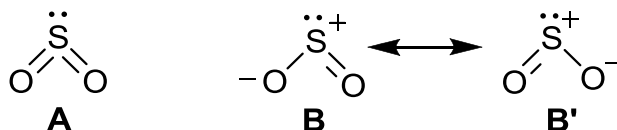


Figure 1.1. Resonance Structures of SO₂.

There are 18 valence electrons in SO₂. The sulfur in SO₂ is sp² hybridized and the oxygens are unhybridized each with the 2s orbital filled.²⁵ The σ M.O. is formed by combining a 2p orbital from each oxygen atoms and two sp² hybridized orbital from the sulfur atom.²⁵ The two bonding orbitals are filled while the two σ* orbitals remain

ⁱ Bond orders were estimated using a variation on Pauling's bond distance-bond order relationship. $D(n') = D1 - 0.997 \log n'$, where n' is the bond order, $D(n')$ is the observed bond length (Å) and $D1$ is the S-O single bond distance extrapolated (1.70 Å). The constant 0.997 was determined by assuming that the bond order of SO in SOF₄ (bond distance = 1.40 Å) is 2.0. Ref: Gillespie, R.J. and Robinson, E.A., *Can. J. of Chem.*, **1963**, *41*, 2074.

unfilled.²⁵ The remaining 10 valence electrons occupy the 3 in plane and 3 out of plane π molecular orbitals. The π bond is formed from a combination of the remaining in plane filled sp^2 hybridized sulfur orbital and two 2p orbital of each of the oxygen atoms (Figure 1.2 **A**).²⁵ All of these 3 π bond molecular orbitals are filled. The remaining 2p orbitals from each oxygen and the 3p orbital from the sulfur form 3 molecular orbitals perpendicular to the plane of SO_2 , two of which are filled (Figure 1.2 **B**).²⁵ This view agrees with the valence bond structures **B/ B'**. Recently, high resolution low temperature X-ray diffraction on crystalline SO_2 was done and bond-order information (B.O = 1.5 and 1.2) was derived using X-ray wavefunction refinement.²³ The conclusion found that bonding in SO_2 was ionic rather than hypervalent.²³

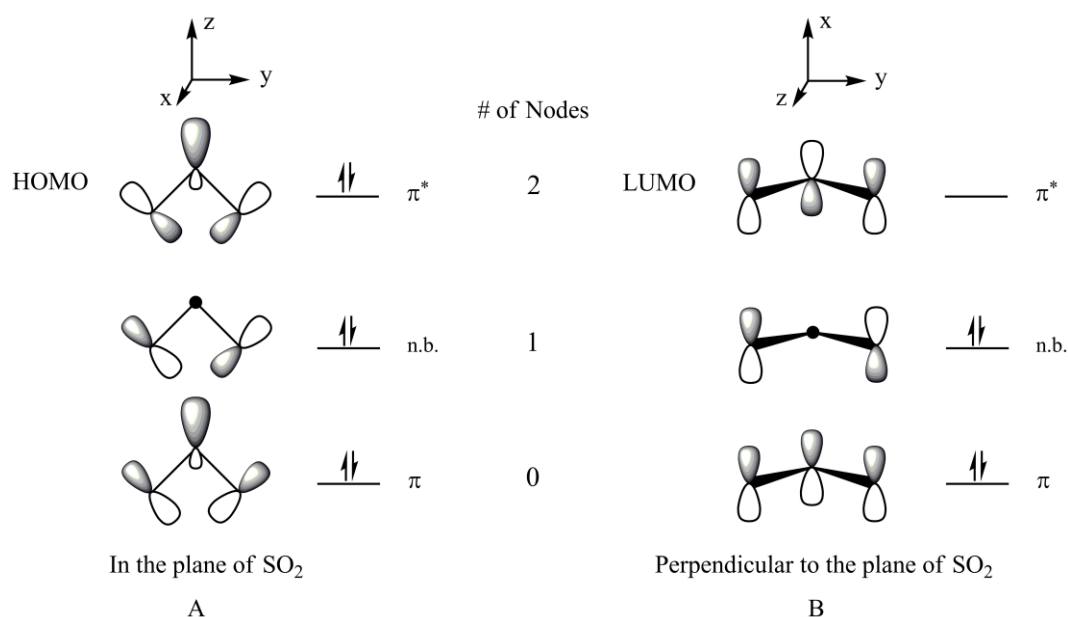


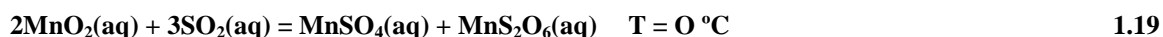
Figure 1.2. SO_2 molecular orbital model of the π systemⁱⁱ. Net π bond order for A = 0 and B = 1.²⁶

ⁱⁱ Relative sizes of orbitals are not shown. Oxygen orbitals are larger than sulfur orbitals in the bonding modes. Sulfur orbitals are larger than oxygen orbitals in the anti-bonding modes.

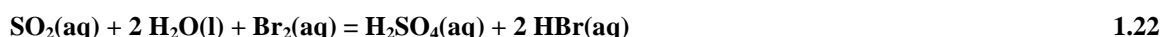
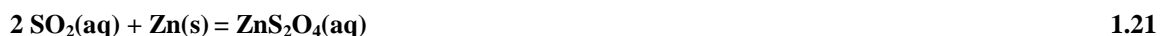
1.2.E. Chemical Properties.

1.2.E.i. Sulfur Dioxide as a Precursor to other Chemicals.

Most SO₂ is used for the production of sulfuric acid, H₂SO₄. Thus if the SO₂ could be recycled then the sulfuric acid industry would benefit.² Sulfur dioxide is also used to produce other chemicals such as sulfites (Eq. **1.18**) and dithionates in aqueous solutions (Eq. **1.19** and **1.20**).² SO₂ can also react with transition metals cations to form transition-metal complexes.²⁷ Chapter 2 discusses another reaction with SO₂ to produce two novel sulfur oxydianions.



Sulfur dioxide can act as an oxidizing agent (Eq. **1.21**) or reducing agent (Eq. **1.22**).^{22,28} In this work, the SO₂ acts as an oxidizing agent in the reactions discussed in Chapter 2.



1.2.E.ii. SO₂ as a Lewis Acid or Lewis Base.

Chemically, sulfur dioxide is an interesting compound since it can act as a Lewis acid or a Lewis base or both simultaneously. A Lewis acid accepts a pair of electrons and a Lewis base donates a pair of electrons. SO₂ acts as a Lewis acid when electrons are accepted into the LUMO (Figure 1.2); SO₂ acts as a Lewis base when electrons are donated from the HOMO π* orbital (Figure 1.2). For example, the SO₂ acts as a Lewis

base in the $\text{BF}_3 \cdot \text{OSO}$ complex and a Lewis acid in the $\text{N}(\text{CH}_3)_3 \cdot \text{SO}_2$ complex.²⁹ Other SO_2 complexes that have O-coordination include $\text{SbF}_5 \cdot \text{OSO}$ and CH_3OSO^+ where SO_2 is the Lewis base.²⁷ SO_2 can also act as both an acceptor and a donor in interactions with metals; electrons can be donated from the HOMO of the SO_2 molecule to an empty metal orbital with the formation of a σ bond and accepted from the filled d orbitals of the metal to the LUMO of the SO_2 (back donation) (eg. in $[\text{M}(\text{SO}_2)_2(\text{PPh}_3)_2]$; $\text{M}=\text{Ni}, \text{Pt}$).³⁰ Sulfur dioxide acts as a Lewis acid in $[\text{N}(\text{CH}_3)_4]_2(\text{SO}_4)(\text{SO}_2)_x$ ($x = 1$ and 2) compounds presented in Chapter 2.

Sulfur dioxide in water acts as a Lewis base and is best represented by equations **1.23** and **1.24**.



According to spectroscopic studies, aqueous SO_2 solutions contains various hydrates, $\text{SO}_2 \cdot x\text{H}_2\text{O}$, based on concentration, temperature and pH.² Therefore, the vigorous anhydrous conditions used in Chapter 2 were crucial to obtain the novel compounds.

1.C. Sulfate Salts.

1.3.A. Naturally Occurring Sulfate Salts.

The second goal of this work is to prepare and identify new sulfur oxyanions, in particular these given on absorption of SO_2 by $[\text{N}(\text{CH}_3)_4]_2\text{SO}_4$ (Chapter 2). Sulfur oxydianions were identified over a century ago; sulfate was the first known sulfur oxydianion (Table 1.1).

Table 1.1. Known Sulfur Oxydianions Containing 1 - 3 Sulfur Atoms in the Solid State.

1	2	3
	$[\text{O}_3\text{S-S}]^{2-}$ 1799 Chaussie $[2\text{Na}^+]$ 1952 Taylor $[2\text{Na}^+]^a$	
	$[\text{O}_2\text{S-SO}_2]^{2-}$ 1825 Berzelius $[2\text{Na}^+]$ 1956 Dunitz $[2\text{Na}^+]^b$	
$[\text{SO}_3]^{2-}$ 1702 Stahl $[2\text{K}^+]$ 1931 Zachariassen $[2\text{Na}^+]^c$	$[\text{O}_3\text{S-SO}_2]^{2-}$ 1797 Vauquelin $[2\text{Na}^+]$ 1932 Zachariassen $[2\text{K}^+]^d$	
	$[\text{O}_3\text{S-SO}_3]^{2-}$ 1819 Gay-Lussac $[\text{Mn}^{2+}]$ 1931 Barnes $[2\text{K}^+]^e$	$[\text{O}_3\text{S-S-SO}_3]^{2-}$ 1841 Langlois $[2\text{K}^+]$ 1934 Zachariassen $[2\text{K}^+]^f$
$[\text{SO}_4]^{2-}$ 1625 Glauber $[2\text{Na}^+]$ 1927 Goeder $[2\text{K}^+/2\text{Rb}^+/2\text{Cs}^+]^g$	$[\text{O}_3\text{S-O-SO}_3]^{2-}$ 1861 Rosenstiehl $[2\text{Na}^+/2\text{K}^+]$ 1960 Truter $[2\text{K}^+]^h$	$[\text{O}_3\text{SOSO}_2\text{OSO}_3]^{2-}$ 1868 Schultz-Sellack $[2\text{Na}^+]$ 1954 Eriks $[2\text{N}_2\text{O}_5^+]^i$
	$[\text{O}_3\text{S-O-O-SO}_3]^{2-}$ 1891 Marshall $[2\text{K}^+]$ 1934 Zachariassen $[2\text{Cs}^+/2\text{NH}_4^+]^j$	

* Oxydianion; Year Discoverer [Counter Cation]³¹; Year Crystallographer [Counter Cation]

^aReference 32. ^bReference 33. ^cReference 34. ^dReference 35. ^eReference 36. ^fReference 37. ^gReference 38. ^hReference 39. ⁱReference 40. ^jReference 41.

Sulfate containing salts are found in some minerals and spring waters. Natural sulfate salts include calcium sulfate (gypsum, $\text{CaSO}_4 \cdot \text{H}_2\text{O}$, and anhydrite, CaSO_4), magnesium sulfate (Epsom salts, $\text{MgSO}_4 \cdot 7\text{H}_2\text{O}$), and kieserite $\text{MgSO}_4 \cdot \text{H}_2\text{O}$), barium sulfate (heavy spar, sparite, BaSO_4), strontium sulfate (celestite, SrSO_4) and sodium sulfate (Glauber's salt, $\text{Na}_2\text{SO}_4 \cdot 10\text{H}_2\text{O}$).²²

In the literature, the sulfate anion has not been identified in the gas phase as it undergoes a Coulombic explosion to give the radical $\text{SO}_4 \cdot^-$.⁴² However, it has been characterized in solution as well as in the solid state.⁴³ The sulfate anion in these two states is stabilized by solvation and lattice energies.⁴⁴

1.3.B. Structure and Bonding in Sulfate Dianion.

The sulfate ion is tetrahedral (T_d) ($S-O: 1.49 \text{ \AA}$)² (Figure 1.3) (eg. K_2SO_4). Even though sulfate has been known for a long time, the bonding in sulfate is still debated. Structure **A** obeys Lewis' octet rule (Figure 1.3 **A**) with all S-O single bond lengths.⁴⁵ Pauling describes SO_4^{2-} as having 2 S-O single bonds and two S-O double bonds delocalized over the SO_4^{2-} (Figure 1.3, Structure **B**, **B'** and **B''**) since the S-O bonds in sulfate are shorter than expected.^{2,46}

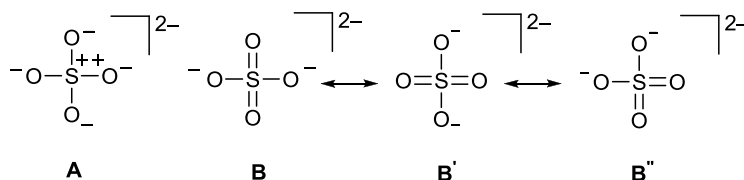


Figure 1.3. Valence Bond Description of the Bonding in Sulfate.

Pauling's view describes sulfur with 12 valence electrons leaving two double bonds and two single bonds to oxygen making sulfur a hypervalent atom, an expansion of the octet.⁴⁶ The hypervalent structure is supported by experimental evidence of the short S-O bond length distance 1.49 \AA ($B.O = 1.62$)^{ii.2} Pauling believed that heavier atoms did not need to obey the octet rule since they could use d-orbitals for bond formation.⁴⁷ In sulfate Pauling argued that the contribution of the empty sulfur atom d-orbitals overlapping with the filled oxygen p orbitals gave rise to $p_\pi-d_\pi$ bonding. However, calculations predict that the d-orbitals are too high in energy to contribute to the bonding.⁴⁸ A general tetrahedral molecular orbital treatment is given in Purcell and Kotz.⁴⁹

The ionic view using various calculations of the S-O bonding have been discussed by the theoreticians Cioslowski and Surjan and also by Dobado et al..^{50,51} A recent view

by Schmøkel et al. views the sulfate as represented by **A** but with the S-O bonding as polar σ bonds mainly characterized by electrostatic interactions.⁴⁸ Multipole modeling of experimental synchrotron X-ray electron diffraction data ($T = 10 \pm 3$ K) on K_2SO_4 fitted their periodic DFT calculations.⁴⁸ The charges on the sulfur atom are higher than expected (exp: 4.27, calc (QTAIM): 3.86) while the charges on some of the oxygen atoms are lower (exp: -1.37 to -1.43 , calc (QTAIM): -1.41 - -1.41).⁴⁸ The findings of the bonding in the sulfate dianion and the crystalline sulfur dioxide (Section 1.2.D) imply that the bonding in sulfur oxygen compounds is more ionic than previously thought.

1.3.C. Simple Sulfate Salts in Water.

The absorption of SO_2 using sulfate salts needs to be a gas solid reaction excluding water. In water (pH = 7), sulfate largely forms bisulfate as shown in equation 1.25.⁵²



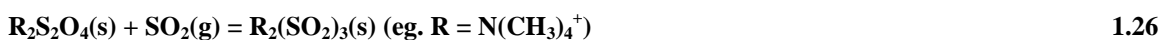
1.3.D. Sulfate + SO_3 .

Sulfate acts as a Lewis base. The addition of $xS_3O_9/3$ to sulfate salts of small cations lead to $S_2O_7^{2-}$ ($x = 1$), $S_3O_{10}^{2-}$ ($x = 2$), $S_4O_{13}^{2-}$ ($x = 3$) and $S_5O_{16}^{2-}$ ($x = 4$).²² The addition of SO_2 to a larger cationic sulfate salt, $[N(CH_3)_4]_2SO_4$, will be discussed in Chapter 2.

1.D. Removal and Recovery of SO_2 under Ambient Conditions by $R_2S_2O_4(s)$ ($R = N(CH_3)_4^+$, $N(C_2H_5)^+$).

Francis LeBlanc calculated the thermodynamics of the reaction of $R_2S_2O_4(s) + SO_2(g)$ in the solid state using F. Grein and P. Bruna's theoretical gas phase calculations

and initially proposed that $R_2S_2O_4$ with large R would absorb and release SO_2 (Eq. **1.26**) (see Supporting Information S.1 for calculating the ΔG in the solid state of the reaction). The absorption and desorption of SO_2 using larger dithionite salts, $R_2S_2O_4$, was estimated to be feasible ($\Delta G = -87$ kJ/mol, $R = N(CH_3)_4^+$).



Various people attempted to prepare salts with large cations over the last 30 years unsuccessfully. There were problems obtaining pure dithionite salts due to the decomposition of the salts containing large cations during the synthesis as well as during the addition and removal of SO_2 . The syntheses of the dithionite salts were done in an aqueous environment promoting decomposition. The addition of the SO_2 to the dithionite salts produced other species such as polythionates. However, recently my colleagues Scott Greer, Tressia Paulose and myself have been able to prepare and fully characterize RS_2O_4 ($R = Me_4N^+$, Et_4N^+ , Me_3EtN^+ , Bu_4N^+ , $PhMe_3N^+$, $(Me_2N)_2CC(NMe_2)_2^{2+}$) and RS_2O_4 ($R = Me_4N^+$, Et_4N^+ , Me_3EtN^+ , Bu_4N^+ , $(Me_2N)_2CC(NMe_2)_2^{2+}$) + SO_2 compounds.²⁶ Since there was a major problem with the dithionite system an alternative sulfur oxyanion, SO_4^{2-} , was examined (Chapter 2). F. Grein and P. Bruna calculated enthalpies and free energy of the addition of sulfur dioxide to sulfate in the gas phase and I determined the thermodynamics in the solid state which was found to be favourable ($\Delta G = -84$ kJ/mol). In addition the starting material, tetramethylammonium sulfate, is commercially available. The reaction of $SO_2(g)$ uptake by $[N(CH_3)_4]_2SO_4(s)$ is given in Chapter 2.

References

1. Pandey, R.; Biswas, R.; Chakrabarti, T.; Devotta, S.; *Critical Reviews in Environmental Science and Technology*, **2005**, *35*, 571.
2. Greenwood, N. N.; Earnshaw, A. *Chemistry of the Elements*, 2nd ed., Pergamon Press: Oxford, UK, 1997.
3. Gerhard, E.R.; Johnstone, H.F. *Industrial and Engineering Chemistry* **1955**, *47*, 972.
4. Gunn, J.; Keller, W.; Negusanti, J.; Potvin, R.; Beckett, P.; Winterhalder, K. *Water, Air and Soil Pollution* **1995**, *85*, 1783.
5. Yu, G.; Chen, X. *J. Phys. Chem. B* **2011**, *115*, 3266.
6. Kettner, H.; *Bull. Eld. Hlth. Org.* **1965**, *32*, 421.
7. Oh, J.J.; LaBarge, M.S.; Matos, J.; Kampf, J.W.; Hillig II, K.W.; Kuczkowski, R.L. *J. Am. Chem. Soc.* **1991**, *113*, 4732.
8. Woodhouse, E.J.; Norris, T.H. *Inorganic Chemistry* **1971**, *10*, 614.
9. Kumar, A.; McGrady, G. S.; Passmore, J.; Grein, F.; Decken, A. *Z. Anorg. Allg. Chem.* **2012**, *638*, 744.
10. Lippincott, R.E.; Welsh, E.F. *Spectrochimica Acta* **1961**, *17*, 123.
11. (a) Shiflett, M.B.; Yokozeki, A. *Energy Fuels*, **2010**, *24*, 1001. (b) Shiflett, M.B.; Yokozeki, A. *Ind. Eng. Chem. Res.* **2010**, *49*, 1370.
12. Anderson, J.L.; Dixon, J.K.; Maginn, E.J.; Brennecke, J.F. *J. Phys. Chem. B*, **2006**, *110*, 15059.
13. Ren, S.; Hou, Y.; Wu, W.; Jin, M. *Ind. Eng. Chem. Res.* **2011**, *50*, 998.

14. Baj, S.; Siewniak, A.; Chrobok, A.; Krawczyk, T.; Sobolewski, A. *J. Chem. Technol. Biotechnol.* **2012**.
15. Britt, D.; Tranchemontagne, D.; Yaghi, O. M. *Proc. Natl. Acad. Sci. U. S. A.*, **2008**, 105, 11623.
16. Elschenbroich, C., Gondrum, R. and Massa, W., *Angewandte Chemie*, **1985**, 97, 976.
17. *Matheson Gas Data Book*, 4th ed., The Matheson Company, Inc.: East Rutherford, NJ, 1966.
18. Waddington, T.C. *Nonaqueous Solvent Systems*, Academic Press: London, 1965.
19. Ross, J.; Percy, J.H.; Brandt, R.L.; Gebhart, A.I.; Mitchell, J.E., Yolles, S. *Industrial and Engineering Chemistry*, **1942**, 32, 924.
20. Elving, P.J.; Markowitz, J.M. *J. Chem. Ed.* **1960**, 37, 75.
21. Sharp, P.R.; Bard, A.J.; *Inorganic Chemistry* **1983**, 22, 3462.
22. Holleman, A.F.; Wiberg, E.; Wiberg, N. *Inorganic Chemistry*, Academic Press: San Diego, USA, 2001.
23. Grabowsky, S.; Luger, P. Bushmann, J.; Schneider, T.; Schirmeister, T.; Sobolev, A.N.; Jayatilaka, D. *Angew. Chem. Int. Ed.* **2012**, 51, 6776.
24. Holder, jr. C.H.; Fink, M. *J. Chem. Phys.* **1981**, 75, 5323.
25. Decken, A.; Knapp, C.; Nikiforov, G.B.; Passmore, J., Rautianinen, J.M.; Wang, X., Zeng, X. *Chem. Eur. J.* **2009**, 15, 6504.
26. Greer, S. (2012). *Towards the Development of New Solid Sorbents for Sulfur Dioxide Sequestration*. Unpublished masters dissertation, University of New Brunswick, Fredericton, NB.

27. Mews, R.; Lork, E.; Wastson, P.G.; Görtler, B. *Coordination Chemistry Reviews* **2000**, *197*, 277.
28. Jolly, W.L. *Modern Inorganic Chemistry*, McGraw-Hill: New York, NY, 1984.
29. Peebles, S.A.; Sun, L.; Kuczkowski, R.L.; Nxumalo, L.M.; Ford, T.A. *Journal of Molecular Structure* **1998**, *471*, 235.
30. Ryan, R. R.; Kubas, G. J.; Moody, D. C.; Eller, P. G. *Struct. Bonding (Berlin)*, **1981**, *46*, 47.
31. Mellor, J.W. *A Comprehensive Treatise on Inorganic and Theoretical Chemistry*, Vol. X, Logmans Green and Co. LTD.: London, UK, 1940 and references within.
32. Taylor, P.G.; Beevers, C.A. *Acta Cryst.* **1952**, *5*, 341.
33. Duniz, J.D. *Acta Cryst.* **1956**, *9*, 579.
34. Zachariasen, W.H.; Buckley, H.E. *Phy. Rev.* **1931**, *37*, 1295.
35. Zachariasen, W.H. *Phy. Rev.* **1932**, *40*, 923.
36. Barnes, W.H.; Helwig, G.V. *Canadian Journal of Research* **1931**, *4*, 565.
37. Zachariasen, W.H. *Z. Kristallogr.* **1934**, *89*, 529.
38. Goeder, F.P. *Proceedings of the National Academy of Sciences of the United States of America* **1927**, *13*, 793.
39. Lynton, H.; Truter M.R. *Journal of the Chemical Society* **1960**, 5112.
40. Eriks, K.; MacGillavry, C. H. *Acta Cryst.* **1954**, *7*, 430.
41. Zachariasen, W.H.; Mooney, R.C.L. *Zeitschrift fuer Kristallographie* **1934**, *88*, 63.
42. Wang, X.B.; Nicholas, J.B.; Wang, L.S. *J. Chem. Phys.* **2000**, *113*, 10837.

43. Grein, F and Chan, J., *Computational & Theoretical Chemistry*, **2011**, 966, 225
and references within.
44. Knapp, C.; Schulz, C. *Chem. Commun.* **2009**, 4991.
45. Lewis, G. N. *J. Am. Chem. Soc.* **1916**, 38, 762–785.
46. Pauling, L. *Journal of Physical Chemistry*, **1952**, 56, 361.
47. Pauling, L. *The nature of the chemical bond*, Cornell University Press: Ithaca, NY, 1939.
48. Schmøkel, M.S.; Cenedese, J.O.; Jørgensen, M.R.V., Chen, Y.S., Gatti, C., Stalke, D., Iversen, B.B. *Inorganic Chemistry*, **2012**, 51, 8607.
49. Purcell, K. F.; Kotz, J. C. *Inorganic Chemistry*, W. B. Saunders Company: Philadelphia, USA, 1977.
50. Cioslowski, J.; Surján, P. R. *J. Mol. Struct. THEOCHEM* **1992**, 87, 9.
51. Dobado, J. A.; Martínez-García, H.; Molina, J. M.; Sundberg, M. R. *J. Am. Chem. Soc.* **1998**, 120, 8461.
52. Irish, D.E.; Chen, H. *J.Chem. Phys.* **1970**, 74, 3796.

Chapter 2. The Synthesis of $[\text{N}(\text{CH}_3)_4]_2\text{O}_3\text{SOSO}_2(\text{s})$ and $[\text{N}(\text{CH}_3)_4]_2[(\text{O}_2\text{SO})_2\text{SO}_2]\cdot\text{SO}_2(\text{s})$ Containing $(\text{SO}_4)(\text{SO}_2)_x^{2-}$ $x = 1, 2$, Members of a New Class of Sulfur Oxydianions

The following chapter presents a publication of a full paper “The Synthesis of $[\text{N}(\text{CH}_3)_4]_2\text{O}_3\text{SOSO}_2(\text{s})$ and $[\text{N}(\text{CH}_3)_4]_2[(\text{O}_2\text{SO})_2\text{SO}_2]\cdot\text{SO}_2(\text{s})$ Containing $(\text{SO}_4)(\text{SO}_2)_x^{2-}$ $x = 1, 2$, Members of a New Class of Sulfur Oxydianions”, P. Bruna, A. Decken, F. Grein, J. Passmore, J. M. Rautiainen, S. Richardson, T. Whidden *Inorganic Chemistry*, **2013**.

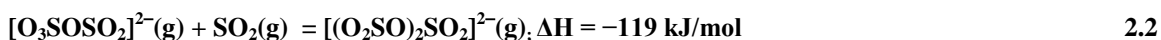
Preparation of $[\text{N}(\text{CH}_3)_4]_2\text{O}_3\text{SOSO}_2(\text{s})$ and $[\text{N}(\text{CH}_3)_4]_2[(\text{O}_2\text{SO})_2\text{SO}_2]\cdot\text{SO}_2(\text{s})$ was carried out by the candidate. Raman and IR spectra were obtained and analyzed by the candidate. TGA/DSC was obtained by the candidate with guidance from Sandra Riley and analyzed by the candidate. The crystal structure was obtained by Dr. Andreas Decken. Quantum chemical calculations were carried out and interpreted by Dr. Fritz Grein. The paper was written by Dr. Mikko Rautiainen, Dr. Tom Whidden and the candidate under the guidance of Dr. Jack Passmore.

2.1. Introduction.

The known salts of binary sulfur oxydianions with one to three sulfur atoms were discovered prior to 1891 (Table 1.1) and are part of the foundational facts of chemistry.¹ Sulfur oxyanions are important in all areas of science and technology, and one would assume that their chemical and physical properties have now been exhaustively established, especially for salts of the first identified hydrated sulfur oxydianion, $[\text{SO}_4]^{2-}$ but this is not the case.² Numerous sulfate salts having small counter cations are

stable in the solid state and several are naturally occurring. However, $[\text{SO}_4]^{2-}$ undergoes a Coulombic explosion in the gas phase, producing an electron and the $[\text{SO}_4]^{-\bullet}$ radical.³

In this paper, synthesis of two new sulfur oxydianions, $[\text{O}_3\text{SOSO}_2]^{2-}$ and $[(\text{O}_2\text{SO})_2\text{SO}_2]^{2-}$, were obtained by addition of one or two SO_2 to the sulfate dianion. $[\text{O}_3\text{SOSO}_2]^{2-}$ is an isomer of the long known $[\text{O}_3\text{SSO}_3]^{2-}$ (Table 1.1) and isoelectronic with $\text{O}_3\text{ClOClO}_2$.⁴ When compared to sulfate the charge repulsion between the two negative charges is reduced in $[\text{O}_3\text{SOSO}_2]^{2-}$ which we surmised is a driving force for reaction **2.1**. In a paper by Chan and Grein³, structures and energies of these new dianions were calculated at the B3PW91-6-311+G(3df) level of theory. Accordingly, in gas phase reaction (Eq. **2.1**) for the formation of $[\text{O}_3\text{SOSO}_2]^{2-}$ and reaction (Eq. **2.2**) for the formation of $[(\text{O}_2\text{SO})_2\text{SO}_2]^{2-}$ were calculated to be exothermic, with ΔH values of -211 and -119 kJ/mol, respectively.



The energetics for the corresponding reactions of solid sulfate salts can be estimated using a Born-Haber cycle for $\text{R}_2\text{SO}_4(\text{s})$ $\text{R} = \text{N}(\text{CH}_3)_4^+$ and Na^+ (Figure 2.1). The lattice enthalpies in the Born-Haber cycle, even for hitherto unknown salts, are readily estimated from the corresponding molecular volumes using volume based thermodynamics (V.B.T.) (See Supporting Information Section S.1).

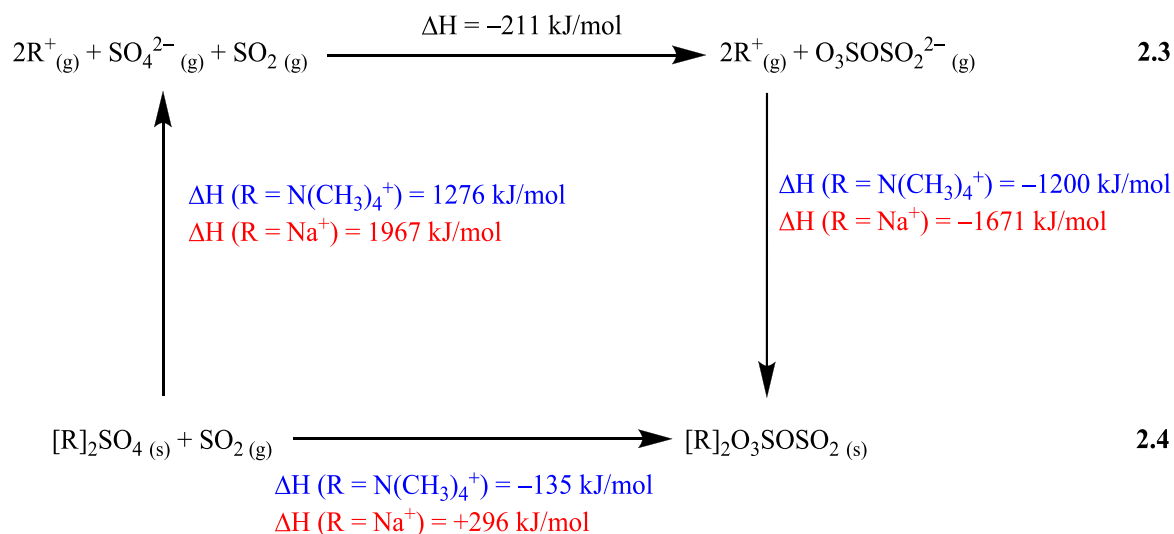


Figure 2.1. Born-Haber cycle for reaction of $\text{R}_2\text{SO}_4(\text{s}) + \text{SO}_2(\text{g})$ where $\text{R} = \text{N}(\text{CH}_3)_4^+$ (blue) and Na^+ (red).

The Born-Haber cycles have been used to determine the free energy curves for the corresponding reactions and the ΔG values account for the facts that solid Na_2SO_4 does not react with $\text{SO}_2(\text{g})$ and that the reaction of $\text{SO}_2(\text{g})$ with solid $[\text{N}(\text{CH}_3)_4]_2\text{SO}_4$ is energetically favourable (Figure 2.1, Section S.1). We have further estimated the free energies for reactions of SO_2 with a variety of sulfate salts having differing cation volumes (Table S.1), as well as for the reaction of SO_2 with $\text{R}_2\text{O}_3\text{SOSO}_2$ according to equation 2.5. These results, shown in Figure 2.2, suggest that reactions 2.4 and 2.5 are favorable for salts of cations having volumes equal to or larger than that of $\text{N}(\text{CH}_3)_4^+$.

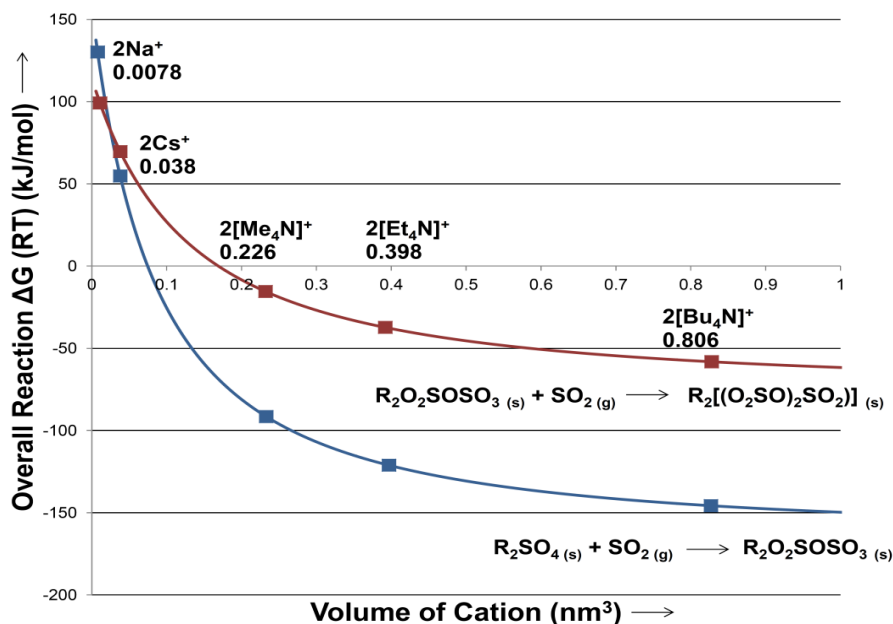


Figure 2.2. Estimated ΔG_{rxn} (298 K) for equation 2.4 and 2.5 as shown below:



Experimental support for the viability of these reactions can be found in a 1938 report by Jander and Mesech⁵ that examined the temperature/vapour pressure characteristics of $[\text{N}(\text{CH}_3)_4]_2\text{SO}_4$ with $\text{SO}_2(\text{g})$. They reported the formation of two solvates $[\text{N}(\text{CH}_3)_4]_2\text{SO}_4 \cdot x\text{SO}_2$ $x = 3, 6$, and that the properties of $[\text{N}(\text{CH}_3)_4]_2\text{SO}_4 \cdot x\text{SO}_2$ $x = 1, 2$ implied a chemical reaction of SO_2 rather than solvate formation.⁵

This work is of both fundamental and practical interest. On the fundamental side, the successful preparation of the two novel oxyanions, $[\text{O}_2\text{S}^{\text{IV}}\text{OS}^{\text{VI}}\text{O}_3]^{2-}$ and $[\text{O}_2\text{S}^{\text{IV}}\text{OS}^{\text{VI}}(\text{O}_3)\text{S}^{\text{IV}}\text{O}_2]^{2-}$, constitutes the discovery of a new class of sulfur oxyanions, $[(\text{SO}_4)(\text{SO}_2)_x]^{2-}$, analogous to the well-known polysulfates $[(\text{SO}_4)(\text{SO}_3)_x]^{2-}$ ($x = 1 - 2$) produced by the addition of $x\text{S}_3\text{O}_9/3$ to salts of SO_4^{2-} (Table 1.1) (also known with $x = 4$ and 5). Furthermore, our theoretical results imply that the chemistry of simple polyanions

of large cations may be very different from that of the well-known salts of smaller cations and that stable salts containing numerous new classes of simple binary oxyanions and related anions can be predicted using our methodology and subsequently prepared and studied. Thus preparation of these novel salts constitutes a valuable confirmation of the predictive ability of our methodology.

Within a more practical context, any materials that reversibly absorb and release SO_2 under ambient or near-ambient conditions (i.e. Eq. 2.4 and Eq. 2.5) are of potential industrial interest. Sulfur dioxide is a by-product of burning fossil fuels, especially coal, and emissions of SO_2 produce acid rain that acidifies water resources, degrades monuments and buildings, and harms plant life. The current industrial methods for SO_2 absorption are energetically inefficient, requiring high temperatures for both absorption and regeneration steps. As well, current methods do not capture all of the SO_2 , with about 5% released into the air.⁶

2.2. Experimental.

2.2.2.A. General Procedures.

All solids were manipulated in an MBraun Unilab drybox under a nitrogen atmosphere and/or using a Monel vacuum line and vapour pressure gauge ($V = 52 \text{ mL}$) and general techniques have been fully described elsewhere.⁷ The reaction vessel used for *in situ* Raman experiments and for vapour pressure measurements (**A**) was a single 1 cm OD Pyrex tube ($V = 14 \text{ mL}$) equipped with a Rotaflo (HP 6K) Teflon-in-glass valve; the vessel used to grow crystals (**B**) was comprised of two 3 cm OD Pyrex tubes connected by a medium glass frit to form a H-shaped vessel equipped with two Rotaflo (HP 6K) Teflon-in-glass valves (Figure S.1). Weights were obtained using either a Mettler PM100

balance (0 - 110 g + 0.001 g capacity) or a Mettler H311 balance (0 - 240 g + 0.0001 g). Vapour pressure measurements were obtained at 20 °C using an Accu-Cal Plus Digital gauge (3D Instruments) with a range of 0 - 1500 + 2.5 mm of Hg.

FT-IR spectra were recorded on a Thermo Nicolet NEXUS 470 FT-IR. Samples were prepared quickly, to minimize decomposition of product, in the glove box and the spectra obtained as Nujol mulls using KBr plates that were wrapped on the outer edges with Teflon tape. FT-Raman spectra were recorded on a Thermo Nicolet 6700 FT-IR equipped with a Thermo Nicolet NXR FT-Raman accessory at 298 K using a Nd:YVO₄ laser (emission wavelength: 1064 nm; 180° excitation). All Raman spectra were obtained *in situ* in vessel **A**. Intensities were integrated from the area under the band. Elemental analyses were performed using a LECO CHNS-932 analyzer.

Thermogravimetric analyses (TGA) and differential scanning calorimetry (DSC) were performed on a TA Instruments Q50 analyzer. For TGA, approximately 5 mg of sample was loaded into an Al crucible and crimped with an Al cover in an argon-filled glovebox. A pinhole pierced in the cover enabled the escape of SO₂ that evolved during the measurement while minimizing the exposure of the sample to the atmosphere as it was transferred to the TGA instrument. The sample was heated to 500 °C at a ramp rate of 5 °C/min under a 120 mL/min N₂ flow. For DSC, 5 mg of material was placed in an Al pan, which was crimped with an Al cover in an argon-filled glovebox. The sample pan was mounted on the instrument and the sample was heated to 500 °C at a rate of 5 °C/min under a N₂ flow of 95 mL/min. The reference sample was an empty Al pan containing a cover.

2.2.2.B. Materials.

Sulfur dioxide (Matheson) was stored over molecular sieves (4 Å) in a 100 mL round bottom flask (rbf) equipped with a Whitey valve for 24 hrs and vacuum distilled to a similar rbf and stored over CaH₂ to guarantee that the SO₂ was dry. The SO₂ was degassed using a freeze, pump, thaw method prior to use and was freshly distilled into the reaction vessel via the vacuum line. Tetramethylammonium sulfate (Aldrich, > 99.0%, white free-flowing powder) was used as received. The high purity of the sulfate salt was confirmed by elemental analysis (Found: %C 39.46, %H 9.47, %N 11.27, %S 13.29; Calculated: %C 39.32, %H 9.90, %N 11.46, %S 13.12) and by vibrational spectroscopy, the spectrum was identical to that reported by Malchus and Jansen.⁸ Tetramethylammonium sulfate (TCI) was dried under vacuum for 24 hrs and shown to be spectroscopically (IR and Raman) and analytically less pure (Found: %C 40.19, %H 9.73, %N 11.26, %S 12.50) compared to the Aldrich sample. The Aldrich sample was the preferred sample and was the one used unless otherwise specified. Paratone-N oil (Hampton Research, clear pale yellow oil) was used as received.

2.2.2.C. X-Ray Crystallography.

A hemisphere of X-ray diffraction data was collected for crystals of [N(CH₃)₄]₂[(O₂SO)₂SO₂²⁻]₂•SO₂ using a Bruker AXS P4/SMART 1000 diffractometer. ω and θ scans had a width of 0.3° and 10 s exposure times. The detector distance was 5 cm. The crystal was twinned and the orientation matrices for two components were determined (CELL_NOW).⁹ The data were reduced (SAINT)¹⁰ and corrected for absorption (TWINABS)¹¹. The structure was solved by direct methods and refined by full-matrix least squares on F²(SHELXTL)¹² on all data. All non-hydrogen atoms were

refined using anisotropic displacement parameters. Hydrogen atoms were included in calculated positions and refined using a riding model. The reflections were of weak intensity and it was not possible to model any disorder in the anion. CCDC 824802 contain the supplementary crystallographic data for this paper. These data can be obtained free of charge from the Cambridge Crystallographic Data Centre via www.ccdc.cam.ac.uk/data_request/cif.

2.2.2.D. Quantum Chemical Calculations.

All calculations were carried out with the Gaussian 03 program package¹³. The B3PW91¹⁴ functional was used with the 6-311+G(3df)¹⁵ basis set for geometry optimization and frequency calculations. Normal modes were visually assigned using ChemCraft¹⁶. There are significant differences between the calculated intensities and the experimental Raman intensities in the region between 1000 cm⁻¹ and 1200 cm⁻¹ where the calculated intensities are overestimated. Similar discrepancies for the problematic S-O vibrations in this region have been observed in other cases.^{17,18}

2.2.2.E. *In situ* Preparation of [N(CH₃)₄]₂O₃SOSO₂(s).

One mole equivalent of SO₂(g) (0.256 g, 4.000 mmol) according to equation 2.4 (**R** = N(CH₃)₄⁺) was expanded into the vacuum line and onto [N(CH₃)₄]₂SO₄(s) (0.970 g, 3.970 mmol) in vessel A. The vapour pressure was 1400 mm Hg, decreasing over 4 hours until it equilibrated at 95 ± 2.5 mm Hg over a partially clumped yellow solid. The remaining SO₂ in the line was condensed into, and isolated in, vessel A, the contents agitated by hand and in a sonic bath (20 °C) leading to a free flowing white homogeneous powder (1.235 g, 4.004 mmol). The vapour pressure measurements were not taken at this point since several experiments showed that the opening and closing of the vessel

affected the amount of time it took for the full conversion to the $[\text{O}_3\text{SOSO}_2]^{2-}$ anion. After a 7 day period *in situ* Raman spectra showed only bands attributable to $[\text{N}(\text{CH}_3)_4]_2\text{O}_3\text{SOSO}_2(\text{s})$ (Figure 2.3, Figure S.3 and Figure S.2), and vapour pressure dropped to 11.0 mm Hg (5 – 11 mm Hg in related experiments). A more detailed account of the preparation of $[\text{N}(\text{CH}_3)_4]_2\text{O}_3\text{SOSO}_2$ is given in Section S.2.1 of the Supporting Information. The IR spectrum is given in Figure S.4 and Figure S.5. A complete vibrational assignment of $[\text{N}(\text{CH}_3)_4]_2\text{O}_3\text{SOSO}_2(\text{s})$ is given in Table S.2. Vibrations assigned to $[\text{O}_3\text{SOSO}_2]^{2-}$ have been compared with the experimental IR vibrations of the isoelectronic $\text{O}_3\text{ClOClO}_2$ and the calculated [B3PW91/6-311+G(3df)] normal modes and intensities of $[\text{O}_3\text{SOSO}_2]^{2-}$ in Table 2.1. The TGA and DSC results are given in Figures S.11 and S.12, respectively.

2.2.2.F. Removal of SO_2 from $[\text{N}(\text{CH}_3)_4]_2\text{O}_3\text{SOSO}_2(\text{s})$.

$[\text{N}(\text{CH}_3)_4]_2\text{O}_3\text{SOSO}_2(\text{s})$ (1.317 g, 4.270 mmol), prepared from $[\text{N}(\text{CH}_3)_4]_2\text{SO}_4(\text{s})$ (1.029 g, 4.213 mmol) according to equation 2.4 ($\mathbf{R} = \text{N}(\text{CH}_3)_4^+$), was subjected to a dynamic vacuum at R.T. Loss of $\text{SO}_2(\text{g})$ was observed by the turbulence of the white powder and weight loss: (0 min/1.317 g, 10 min/1.270 g, 30 min/1.202 g, 50 min/1.129 g, 90 min/1.042 g, 100 min/1.032 g), as illustrated in Figure S.8. After 100 minutes the Raman spectrum and weight (1.032 g) were, within experimental error, that of the original starting material, $[\text{N}(\text{CH}_3)_4]_2\text{SO}_4(\text{s})$ (1.029 g) (Figure S.9). However, we note that samples of $[\text{N}(\text{CH}_3)_4]_2\text{O}_3\text{SOSO}_2(\text{s})$ (0.149 g) prepared from $[\text{N}(\text{CH}_3)_4]_2\text{SO}_4(\text{s})$ (0.116 g) and $\text{SO}_2(\text{g})$ (0.033 g) isolated in vessel A with the valve closed for 3 - 4 weeks did not lose weight on pumping for one day, but heating to 100 °C for a few minutes led to SO_2

loss and complete recovery of $[\text{N}(\text{CH}_3)_4]_2\text{SO}_4(\text{s})$ (0 min/0.149 g, 10 min/0.119 g), as shown by Raman spectroscopy.

2.2.2.G. Preparation of Crystals of $[\text{N}(\text{CH}_3)_4]_2(\text{O}_2\text{SO})_2\text{SO}_2 \cdot \text{SO}_2(\text{s})$.



Approximately 13 mole equivalents of $\text{SO}_2(\text{g})$ (1.225 g, 19.122 mmol) were condensed directly onto $[\text{N}(\text{CH}_3)_4]_2\text{SO}_4(\text{s})$ (0.369 g, 1.510 mmol) in the LHS of vessel **B** (Figure S.1.). Upon warming to RT a yellow solution was formed. The vessel was evacuated by slowly opening the valve on the LHS of the vessel under dynamic vacuum. Pumping on the yellow solution gave clear colorless crystals in less than 2 minutes. The LHS of the vessel was isolated as soon as crystals were observed with small amounts of liquid remaining. The vessel was transferred to the drybox and clear, colorless crystals suitable for X-ray diffraction were collected using a spatula tip coated with Paratone-N oil. These crystals were placed in a vial under Paratone-N oil for transportation. The vial lid was wrapped with Teflon tape during transportation. Single crystals coated in Paratone-N oil were mounted using a polyimide MicroMount and cooled to $-100\text{ }^\circ\text{C}$ in the cold nitrogen stream of the goniometer. Crystallographic details are given in Table S.4. Figures depicting structures were obtained using the Diamond 3.1 program.

2.2.2.H. Attempted Preparation of $[\text{N}(\text{CH}_3)_4]_2(\text{O}_2\text{SO})_2\text{SO}_2(\text{s})$ from $[\text{N}(\text{CH}_3)_4]_2\text{SO}_4(\text{s})$ and $x\text{SO}_2$ ($x > 2$).



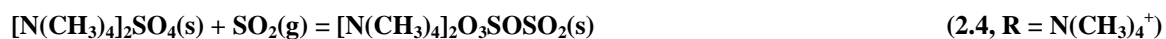
In accordance with equation 2.7, 2.07 mole equivalents of SO_2 (0.233 g, 3.637 mmol) were expanded into the vacuum line and condensed at $-196\text{ }^\circ\text{C}$ onto the white $[\text{N}(\text{CH}_3)_4]_2\text{SO}_4(\text{s})$ (0.430 g, 1.750 mmol) in vessel **A**. Upon warming to RT, a yellow

clumped solid was observed. The contents were agitated by hand and in a sonic bath (20 °C), but the powder never became homogeneous. Several *in situ* Raman spectra were taken over a period of one month. The bands in the spectrum were assigned to $\text{N}(\text{CH}_3)_4^+$, $[(\text{O}_2\text{SO})_2\text{SO}_2]^{2-}$ as well $[\text{O}_3\text{SOSO}_2]^{2-}$ and SO_2 of solvation (Figure S.10). The observed Raman bands attributed to $[(\text{O}_2\text{SO})_2\text{SO}_2]^{2-}$ are compared with the calculated [B3PW91/6-311+G(3df)] normal modes and intensities in Table 2.2. A complete listing of the Raman frequencies has been given in Table S.5 in the Supporting Information. Very similar Raman spectra were obtained from reactions of $[\text{N}(\text{CH}_3)_4]_2\text{SO}_4(\text{s})$ with slightly higher and lower amounts of $\text{SO}_2(\text{g})$ than 2 mole equivalents. Bands attributed to $[(\text{O}_2\text{SO})_2\text{SO}_2]^{2-}$ were also observed in the preparation of $[\text{N}(\text{CH}_3)_4]_2\text{O}_3\text{SOSO}_2(\text{s})$ prior to completion of the reaction (Figure S.3).

The addition of 3.3 mole equivalents of SO_2 to $[\text{N}(\text{CH}_3)_4]_2\text{SO}_4(\text{s})$ (0.430 g, 1.750 mmol) in vessel **A** gave a partly yellow and clumped solid. The contents were agitated at RT by hand and in a sonic bath (20 °C) but the powder never became homogeneous. *In situ* Raman spectra of solids obtained from the reactions $[\text{N}(\text{CH}_3)_4]_2\text{SO}_4 + x\text{SO}_2(\text{g})$ $x = 2.95, 3.30, 5.50$ as a function of time were all similar, except that bands attributed to SO_2 of solvation increased in intensity as the amount of $\text{SO}_2(\text{g})$ reactant increased.

2.3. Results and Discussion

2.2.3.A. The Reversible Absorption of $\text{SO}_2(\text{g})$ by $[\text{N}(\text{CH}_3)_4]_2\text{SO}_4(\text{s})$ with Quantitative Formation of $[\text{N}(\text{CH}_3)_4]_2\text{O}_3\text{SOSO}_2(\text{s})$.



The vapour pressure of one mole equivalent of $\text{SO}_2(\text{g})$ over $[\text{N}(\text{CH}_3)_4]_2\text{SO}_4(\text{s})$ dropped from 1400.0 mm Hg (0 h) to 95.0 mm Hg (4 h), and a much reduced rate of SO_2 uptake

occurred until after 7 days by which time the vapour pressure had decreased to ca. 11.0 mm Hg. The resulting white free flowing powder was unambiguously characterized as $[\text{N}(\text{CH}_3)_4]_2\text{O}_3\text{SOSO}_2$ by *in situ* Raman and IR spectroscopy (see Section 3.3), with the weight gain corresponding to the uptake of one mole equivalent of $\text{SO}_2(\text{g})$ according to equation 2.4, $\mathbf{R} = \text{N}(\text{CH}_3)_4^+$. Quantitative loss of SO_2 occurred on evacuation of freshly prepared samples, with full recovery of $[\text{N}(\text{CH}_3)_4]_2\text{SO}_4(\text{s})$ (Figure S.9, 1.317 g to 1.032 g, theoretical 1.033 g). Periodic *in situ* Raman spectra of the sample were obtained over time (between 4 h and 7 days) prior to full conversion to $[\text{N}(\text{CH}_3)_4]_2\text{O}_3\text{SOSO}_2(\text{s})$ showing strong bands due to the final product and weaker bands attributed to the SO_2 of solvation, $[(\text{O}_2\text{SO})_2\text{SO}_2]^{2-}$ and SO_4^{2-} (Figure S.3). Attempted optimizations of gas phase $(\text{SO}_4)^{2-} \cdot \text{SO}_2$ resulted in the covalently bound $[\text{O}_3\text{SOSO}_2]^{2-}$ structure, suggesting that the SO_2 of solvation is likely associated with $[\text{N}(\text{CH}_3)_4]_2\text{O}_3\text{SOSO}_2(\text{s})$ and/or $[\text{N}(\text{CH}_3)_4]_2(\text{O}_2\text{SO})_2\text{SO}_2(\text{s})$ but not SO_4^{2-} .

2.2.3.B. TGA Analysis of $[\text{N}(\text{CH}_3)_4]_2\text{O}_3\text{SOSO}_2$.

The quantitative loss of SO_2 from $[\text{N}(\text{CH}_3)_4]_2\text{O}_3\text{SOSO}_2(\text{s})$ according to equation 2.4, $\mathbf{R} = \text{N}(\text{CH}_3)_4^+$ on evacuation was consistent with thermogravimetric (TGA) and differential scanning calorimetry (DSC) analyses of this material that showed quantitative loss of SO_2 at approximately 90 °C. At temperatures greater than 90 °C the remaining material exhibited characteristics identically to those of $[\text{N}(\text{CH}_3)_4]_2\text{SO}_4$ as reported by Malchus and Jansen (DTA measurements)⁸ (Figure S.11 and Figure S.12). Over time when $[\text{N}(\text{CH}_3)_4]_2\text{O}_3\text{SOSO}_2$ was stored in a vial in the glovebox, there was a weight loss consistent with the loss of SO_2 . A TGA held at constant RT over a period of

approximately 200 minutes suggested that SO₂ was gradually released under ambient conditions (Figure S.13).

2.2.3.C. The Characterization of [O₃SOSO₂]²⁻ in [N(CH₃)₄]₂O₃SOSO₂(s) by Vibrational Spectroscopy.

The experimental Raman and IR spectra of [N(CH₃)₄]₂O₃SOSO₂ are given in Figure 2.3 and S.4, respectively, with frequency assignments attributable to [O₃SOSO₂]²⁻ given in Table 2.1. Cation bands were assigned by comparison with the previously assigned N(CH₃)₄⁺ in [N(CH₃)₄]₂SO₄.⁸ The experimental data related to the anion is in good agreement with the calculated values and assignments in Table 2.1. 18 bands are expected for a [O₃SOSO₂]²⁻ anion having C_s symmetry, of which 15 were experimentally observed in the Raman spectrum. The remaining 3 bands were calculated to be very weak in intensity or in the low unobservable frequency range. Similar results were seen in the IR, as shown in Figure S.4 and Table 2.1. The anion bands of [O₃SOSO₂]²⁻ are very different and contain more bands from those reported for the well known dithionate anion¹⁹, [O₃SSO₃]²⁻, which is calculated (B3PW91/6-311+G(3df)) to be 53 kJ/mol lower in energy. The IR bands assigned to [O₃SOSO₂]²⁻ are consistent with reported values for the isoelectronic O₃ClOClO₂⁴ (Table 2.1 and Table S.3), further supporting anion identification.

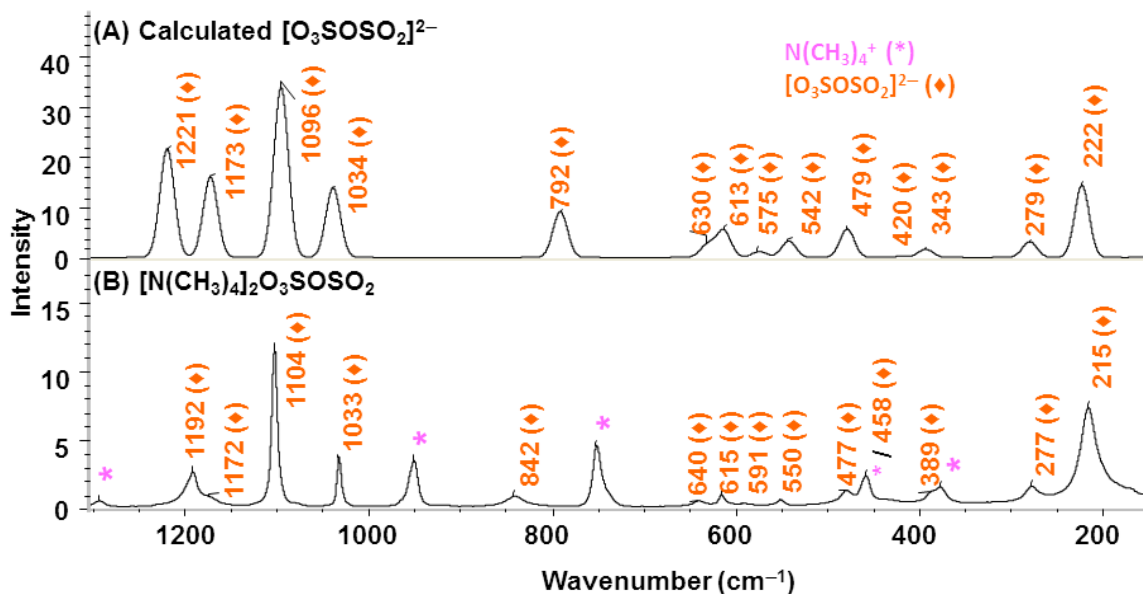


Figure 2.3. The Raman spectrum of [N(CH₃)₄]₂[O₃SOSO₂](s) (B) compared with the calculated (B3PW91/6-311+G(3df)) Raman spectrum of [O₃SOSO₂]²⁻(g) (A) in the 140 - 1500 cm⁻¹ region. Scans: 2048; resolution: 4cm⁻¹; laser power: 0.205 W; Ge detector. Spectra of the 1500-3500 cm⁻¹ region included in Figure S.2. Assignments related to N(CH₃)₄⁺ and SO₄²⁻ were made by comparison with those in [N(CH₃)₄]₂SO₄(s) and SO₂ of solvation with similar compounds found in Table S.6.

Table 2.1. The experimental vibrational spectrum (frequencies cm^{-1} , relative intensities in brackets) of $[\text{O}_3\text{SOSO}_2]^{2-}$ in $[\text{N}(\text{CH}_3)_4]_2\text{O}_3\text{SOSO}_2(\text{s})$, compared with the calculated (B3PW91/6-311+G(3df)) spectrum and the isolectronic $\text{O}_3\text{ClOClO}_2(\text{g})$.^{a,4}

Bands attributed to $[\text{O}_3\text{SOSO}_2]^{2-}$ in $[\text{N}(\text{CH}_3)_4]_2\text{O}_3\text{SOSO}_2(\text{s})$ ^b		Calculated [B3PW91/6-311+G(3df)] gas phase of $[\text{O}_3\text{SOSO}_2]^{2-}$ ^b		$\text{O}_3\text{ClOClO}_2$ Gas phase ^{c,d,4}	Assignments ^e
Raman	IR	Raman	IR	IR	
		35 (1)	35 (<1)		A''
		45 (<1)	45 (1)		A''
		132 (3)	132 (1)		A' $\nu(\text{O}_2\text{S-O})$
215 (84)		222 (42)	222 (13)		A'' $\rho(\text{SO}_2)$ $\rho(\text{SO}_3)$
277 (15)		279 (9)	279 (<1)		A' $\rho(\text{SO}_2)$ $\rho(\text{SO}_3)$
389 (9)	380 (12)	393 (4)	393 (18)		A'' $\delta_{\text{as}}(\text{SO}_3)$
	429 (3)	420 (1)	420 (<1)		A' $\delta_{\text{s}}(\text{SO}_3)$ $\delta(\text{SO}_2)$
477 (10)	476 (9)	479 (17)	479 (40)	544.0	A' $\delta(\text{SO}_3)$ $\delta(\text{SO}_2)$
550 (3)	549 (5)	542 (10)	542 (1)		A'' $\rho_{\text{r}}(\text{SO}_3)$
591 (2)	590 (14)	575 (3)	575 (5)	579.0	A' $\rho(\text{SO}_3)$ $\delta(\text{SO}_2)$ $\nu(\text{O}_2\text{S-O})$
615 (3)	614 (15)	613 (16)	613 (2)	629.0	A' $\nu(\text{O}_2\text{S-O})$ $\delta(\text{SOS})$ $\delta_{\text{as}}(\text{SO}_3)$
640 (3)	634 (21)	630 (8)	630 (48)	691.0	A' $\nu_{\text{s}}(\text{O}_3\text{S-O})$
842 (7)	836 (100)	792 (27)	792 (84)	1024.0	A' $\nu_{\text{s}}(\text{SO}_3)$ $\nu_{\text{s}}(\text{SO}_2)$
1033 (9)	1032 (47)	1039 (41)	1039 (53)	1080.0	A' $\nu_{\text{s}}(\text{SO}_2)$ $\nu_{\text{s}}(\text{SO}_3)$
1104 (37)	1103 (23)	1096 (100)	1096 (10)		A'' $\nu_{\text{as}}(\text{SO}_2)$ $\nu_{\text{as}}(\text{SO}_3)$
1172 (3)	1168 (58)	1173 (47)	1173 (45)		A'' $\nu_{\text{as}}(\text{SO}_3)$
1192 (19)	1210 (87)	1221 (52)	1221 (76)	1265.0	A' $\nu_{\text{as}}(\text{SO}_3)$
1192 (19)	1210 (87)	1222 (12)	1222 (100)	1265.0	$\nu_{\text{as}}(\text{SO}_2)$

^aA full listing of IR and Raman frequencies are given in Table S.2 respectively.

^bbands were assigned visually with the aid of ChemCraft; ν - stretching, δ - bending, ρ - twisting/rocking/wagging

^cA more complete comparison of $\text{O}_3\text{SOSO}_2^{2-}$ and $\text{O}_3\text{ClOClO}_2(\text{g})$ ⁴ and in solid matrices is given in Table S.3.

^dIntensities were not reported.⁴

^eVibration listed first is the main contributor with secondary contribution given on the second line. Equal contributions given on same line.

2.2.3.D. The Structure and Bonding in $[\text{O}_3\text{SOSO}_2]^{2-}$.

The excellent agreement between the experimental and calculated vibrational spectra of $[\text{O}_3\text{SOSO}_2]^{2-}$ strongly supports the validity of the calculated (B3PW91/6-311+G(3df)) structure (Figure 2.4).

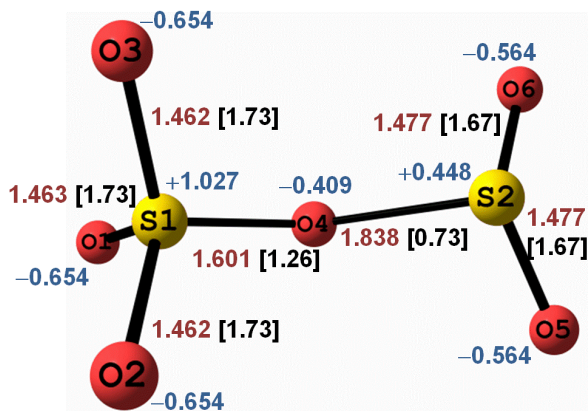


Figure 2.4. Calculated (B3PW91/6-311+G(3df)) structure of $[\text{O}_3\text{SOSO}_2]^{2-}$ in the gas phase; bond lengths (Å) (red), [bond orders] (black) and Mulliken charges (blue).¹ $\angle\text{O2-S1-O1}$: 113.06, $\angle\text{O1-S1-O3}$: 113.06, $\angle\text{O3-S1-O4}$: 107.29, $\angle\text{O4-S1-O2}$: 107.29, $\angle\text{S1-O4-S2}$: 121.88, $\angle\text{O4-S2-O6}$: 100.26, $\angle\text{O6-S2-O5}$: 111.40, $\angle\text{O5-S2-O4}$: 100.26.

The calculated bond lengths, angles and atomic charge in $[\text{O}_3\text{SOSO}_2]^{2-}$ are as expected by comparison with those calculated for the related species, SO_2 , SO_4^{2-} and O_2SOH^- (Figure 2.5). We note that salts of O_2SOH^- are unknown, but evidence has been provided that they exist in aqueous solutions.²⁰

¹ Bond orders were estimated using a variation on Pauling's bond distance-bond order relationship. $D(n') = D1 - 0.997 \log n'$, where n' is the bond order, $D(n')$ is the observed bond length (Å) and $D1$ is the S-O single bond distance extrapolated (1.70 Å). The constant 0.997 was determined by assuming that the bond order of SO in SOF_4 (bond distance = 1.40 Å) is 2.0. Ref: Gillespie, R.J. and Robinson, E.A., *Can. J. of Chem.*, 1963, 41, 2074.

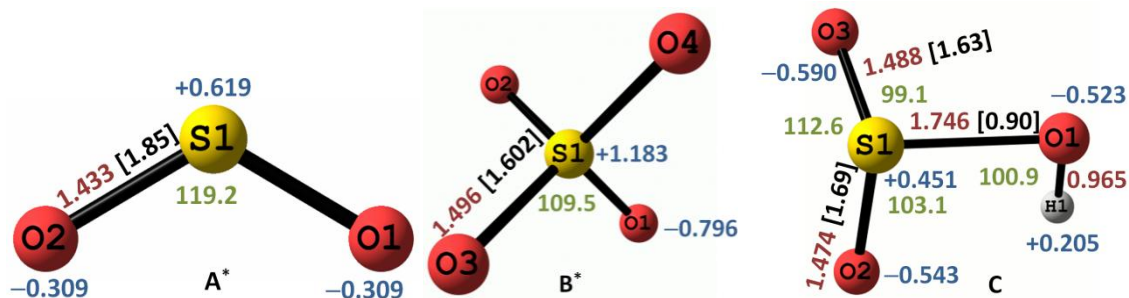


Figure 2.5. A comparison of calculated (B3PW91/6-311+G(3df)) bond lengths, bond angles, bond order and charge in SO_2 (A), SO_4^{2-} (B) and HOSO_2^{2-} (C); bond lengths (Å) (red), bond orders (black), bond angles (green) and Mulliken charges (blue).

*Experimental bond lengths and angles for SO_4^{2-} in $[\text{N}(\text{CH}_3)_4]_2\text{SO}_4(\text{s})^8$, S-O (Å): 1.461(2), $\angle\text{OSO}$ (°): 109.51(9), 109.4(2) and $\text{SO}_2(\text{s})^{21}$, S-O (Å): 1.4297(7), $\angle\text{OSO}$ (°): 117.5(1). Calculated (B3LYP/6-31G(2df,p)) bond lengths of $[\text{O}_2\text{SOH}]^{2-}$, S-O (Å): 1.494, 1.482, 1.768, O-H (Å): 96.6.

The S-O bridging bond lengths (1.601 Å and 1.838 Å) in $[\text{N}(\text{CH}_3)_4]_2\text{O}_3\text{SOSO}_2$ are longer than most other known S-O bond lengths (Figure S.14). The charge transfer to SO_2 in $[\text{O}_3\text{SOSO}_2]^{2-}$ is calculated to be somewhat less than that in $[\text{HOSO}_2]^-$ (0.48 electrons) making SO_4^{2-} a weaker base toward SO_2 than OH^- . In valence bond terms the structure can be represented by valence bond structures **A** (which assumes full electron pair donation from SO_4^{2-} to SO_2) and **B** shown in Figure 2.6.

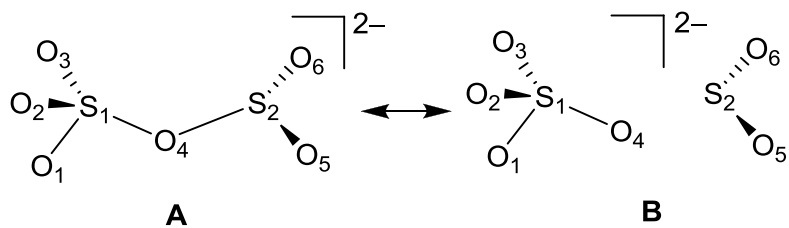


Figure 2.6. A valence bond description of $[\text{O}_3\text{SOSO}_2]^{2-}$.

The addition of SO_2 to SO_4^{2-} can be viewed as proceeding by donation of an electron pair from a negatively charged oxygen atom on the Lewis base SO_4^{2-} , to the positively charged sulfur of the Lewis acid SO_2 , via the π^* SO_2 LUMO perpendicular to the molecular plane.¹⁷ This may account for the formation of the observed $[\text{O}_3\text{SOSO}_2]^{2-}$

rather than the slightly more stable (53 kJ/mol) (B3PW91/6-311+G(3df)) $[\text{O}_3\text{SSO}_3]^{2-}$ isomer. Our calculations indicate that 0.68ⁱⁱ electrons are transferred from SO_4^{2-} to SO_2 thus delocalizing the negative charge and contributing to the driving force of reaction **2.1**. The S-O bond order in the bridging S1-O4 bond (B.O: 1.26) is approximately double that of the similarly bridging S2-O4 bond (B.O: 0.73); the overall charges on the SO_2 unit (O5S2O6; +0.448) and the SO_4 unit (O1O2S1O3O4; +1.027) in $[\text{O}_3\text{SOSO}_2]^{2-}$ imply a relative weighting of the V.B. structures A vs. B of approximately 1 to 2.

2.2.3.E. Preparation of crystals of $[\text{N}(\text{CH}_3)_4]_2(\text{O}_2\text{SO})_2\text{OSO}_2\cdot\text{SO}_2(\text{s})$.

Single crystals of $[\text{N}(\text{CH}_3)_4]_2(\text{O}_2\text{SO})_2\text{SO}_2\cdot\text{SO}_2$ were obtained from a solution of $[\text{N}(\text{CH}_3)_4]_2\text{SO}_4$ dissolved in liquid sulfur dioxide on removal of the solvent. The structure of this salt was unambiguously determined by X-ray crystallography Figure 2.7. This is an SO_2 of solvation of the $(\text{O}_2\text{SO})_2\text{SO}_2^{2-}$ dianion and not the discrete molecule, $(\text{O}_2\text{SO})_2(\text{SO}_2)_2^{2-}$ (see Figure 2.9). We estimated that the formation of $[\text{N}(\text{CH}_3)_4]_2(\text{O}_2\text{SO})_2(\text{SO}_2)_2(\text{s})$ from $\text{N}(\text{CH}_3)_4\text{SO}_4(\text{s})$ is thermodynamically unfavourable.

ⁱⁱ Sum of charge on SO_2 unit (O5S2O6) is 0.68 in comparison with a neutral SO_2 molecule, therefore 0.68 electrons transferred from the SO_4 unit (O1O2S1O3O4) to the SO_2 unit (O5S2O6).

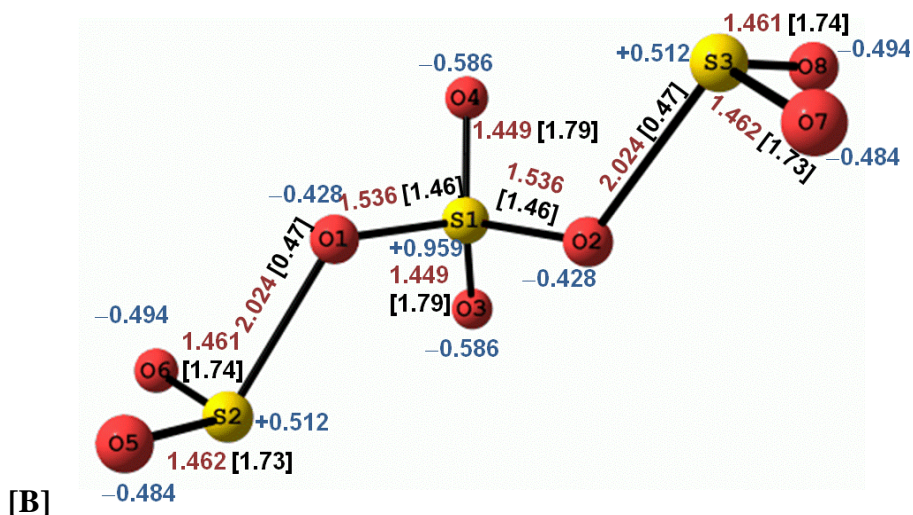
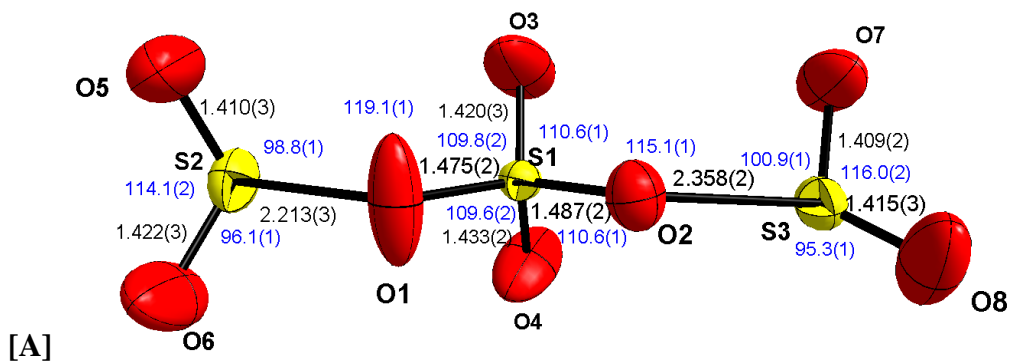


Figure 2.7. [A] Diamond depiction of $[(O_2SO)_2SO_2]^{2-}$ in $[N(CH_3)_4]_2(O_2SO)_2SO_2 \cdot SO_2(s)$ (thermal ellipsoid plots are at the 50% probability level). Bond length (Å) (black) and bond angles (°) (blue). [B] Calculated structure of $[(O_2SO)_2SO_2]^{2-}$ in gas phase; bond lengths (Å) (grey), bond orders (black), and Mulliken charges (blue).¹ Select bond angles (°): $\angle O_5-S_2-O_6$: 113.1, $\angle O_6-S_2-O_1$: 101.1, $\angle O_1-S_2-O_5$: 97.8, $\angle S_2-O_1-S_1$: 122.6, $\angle O_1-S_1-O_3$: 109.7, $\angle O_3-S_1-O_4$: 115.9, $\angle O_4-S_1-O_2$: 109.7, $\angle O_2-S_1-O_1$: 105.7, $\angle S_1-O_2-S_3$: 122.6, $\angle O_2-S_3-O_8$: 101.1, $\angle O_8-S_3-O_7$: 113.1, $\angle O_7-S_3-O_2$: 97.8.

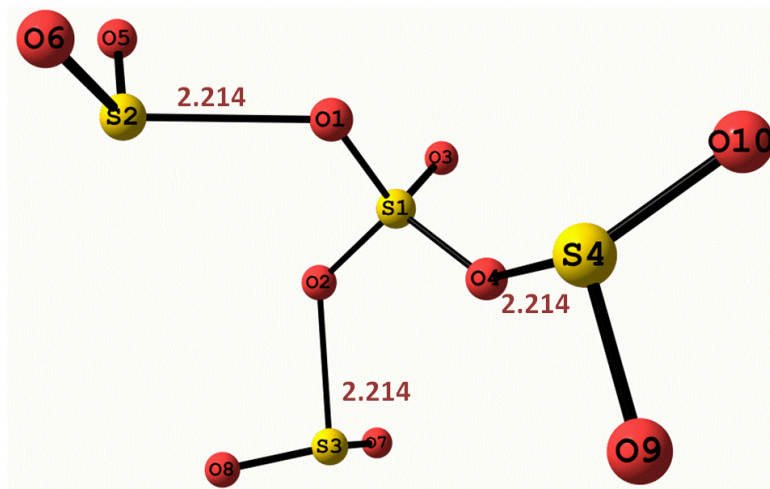


Figure 2.8. Calculated (B3PW91/6-31+G*) structure of $(O_2SO)_2(SO_2)_2^{2-3}$.

The Raman spectrum of very small crystals obtained from the reaction of $[\text{N}(\text{CH}_3)_4]_2\text{SO}_4$ and 2.07 mole equivalents of SO_2 was very similar to those obtained from other reactions with differing molar ratios of the reactants. The main difference in the Raman spectra was the increase in the intensity of SO_2 solvent band as the ratio of SO_2 reactant increased. The peaks in the Raman spectra attributed to $[(\text{O}_2\text{SO})_2\text{OSO}_2]^{2-}$ are compared with the calculated normal modes and intensities in Table 2.2. We were unable to prepare pure samples of $[\text{N}(\text{CH}_3)_4]_2(\text{O}_2\text{SO})_2\text{OSO}_2(\text{s})$ or $[\text{N}(\text{CH}_3)_4]_2(\text{O}_2\text{SO})_2\text{OSO}_2 \cdot \text{SO}_2(\text{s})$. All attempts to prepare the salts gave mixtures as demonstrated by Raman spectroscopy (eg. see Figure S.10).

Table 2.2. The experimental vibrational spectrum (frequencies cm^{-1} , relative intensities in brackets) attributed to $[(\text{O}_2\text{SO})_2\text{SO}_2]^{2-}$ in the solid obtained from the addition of 2.07 mole equivalent of SO_2 to 1 mole of $[\text{N}(\text{CH}_3)_4]_2\text{SO}_4(\text{s})$, compared with the calculated (B3PW91/6-311+G(3df)) spectrum of $[(\text{O}_2\text{SO})_2\text{SO}_2]^{2-}$.^a

$[\text{N}(\text{CH}_3)_4]_2[(\text{O}_2\text{SO})_2\text{SO}_2] \cdot \text{SO}_2(\text{s})$ Raman ^{b,c}	Calculated Raman [(B3PW91/6-311+G(3df)) $[(\text{O}_2\text{SO})_2\text{SO}_2]^{2-}$] ^b	Tentative Assignments ^d
169 sh	161 (19)	B $\nu_{\text{as}}(\text{O}_2\text{S}^{\text{VI}}(-\text{OSO}_2)_2)$
181 (98)	161 (6)	B $\nu_{\text{as}}(\text{O}_2\text{S}^{\text{VI}}(-\text{OSO}_2)_2)$
--	232 (4)	A $\rho_t(\text{SO}_2)$
242 sh (40)	243 (4)	B $\rho_t(\text{SO}_2)$ $\rho_t(\text{SO}_4)$
342 (<1)	367 (0.8)	A $\delta(\text{SO}_4)$ $\rho_w(\text{SO}_2)$
354 (<1)	381 (<1)	B $\rho_w(\text{SO}_2)$
459 (24)	398 (1)	A $\delta(\text{SO}_4)$ $\rho_w(\text{SO}_2)$
496 (7)	492 (17)	A $\delta(\text{O}_2\text{S}^{\text{VI}}(-\text{OSO}_2)_2)$ $\delta(\text{SO}_2)$
544 (5)	541 (<1)	B $\delta(\text{SO}_2)$ $\delta(\text{SO}_4)$
564 (<1)	564 (2)	A $\delta(\text{SO}_2)$ $\delta(\text{SO}_4)$
578 (<1)	586 (8)	A $\delta(\text{SO}_4)$ $\delta(\text{SO}_2)$
593 (<1)	595 (2)	B $\delta(\text{SO}_4)$ $\delta(\text{SO}_2)$
619 (7)	633 (1)	B $\delta(\text{SO}_4)$ $\delta(\text{SO}_2)$
900 (19)	894 (16)	A $\nu_{\text{sym}}(\text{SO}_4)$ $\nu_{\text{sym}}(\text{SO}_2)$
925 (7)	912 (2)	B $\nu_{\text{as}}(\text{SO}_4)$ $\nu_{\text{sym}}(\text{SO}_2)$
1124 (100)	1121 (56)	A $\nu_{\text{sym}}(\text{SO}_2)$; $\nu_{\text{sym}}(\text{SO}_4)$
	1133 (2)	B $\nu_{\text{sym}}(\text{SO}_2)$
1145 (64)	1158 (100)	A $\nu_{\text{sym}}(\text{SO}_4)$ $\nu_{\text{sym}}(\text{SO}_2)$
1238 (5)	1245 (29)	B $\nu_{\text{as}}(\text{SO}_2)$ $\nu_{\text{as}}(\text{SO}_4)$
1249 (2)	1250 (14)	A $\nu_{\text{as}}(\text{SO}_2)$ $\nu_{\text{as}}(\text{SO}_4)$
1294 (7)	1288 (26)	B $\nu_{\text{as}}(\text{SO}_4)$ $\nu_{\text{as}}(\text{SO}_2)$

^aA full listing of IR and Raman frequencies are given in Table S.5 respectively. The observed symmetry is C_1 while that of the calculated anion is C_2 (Figure 2.7).

^bbands were assigned visually with the aid of ChemCraft; ν - stretching, δ - bending, ρ - twisting/rocking/wagging

^cTen of the calculated (B3PW91/6-311+G(3df)) expected 27 vibrations were observed experimentally while eight (12 cm^{-1} (A), 13 cm^{-1} (B), 29 cm^{-1} (A), 48 cm^{-1} (B), 110 cm^{-1} (A), 110 cm^{-1} (B), 161 cm^{-1} (A), 161 cm^{-1} (B)) were too low in frequency to be observed. The remaining 9 calculated vibrations (169 cm^{-1} (B),

342 cm⁻¹ (A), 354 cm⁻¹ (B), 459 cm⁻¹ (A), 496 cm⁻¹ (A), 564 cm⁻¹ (A), 578 cm⁻¹ (A), 593 cm⁻¹ (B), 1294 cm⁻¹ (B)) had very low calculated intensities and therefore were not observed or were buried in cation or other anion bands.

^dAssignments listed first is the main contributor with secondary contribution given on the second line. Equal contribution given on same line.

2.2.3.F. X-ray Structure of [N(CH₃)₄]₂(O₂SO)₂SO₂•SO₂(s).

The structure of [N(CH₃)₄]₂(O₂SO)₂SO₂•SO₂(s) consists of discrete N(CH₃)₄⁺ cations (Figure S.15) and [(O₂SO)₂SO₂]²⁻ anions (Figure 2.7A) which weakly interact with an SO₂ molecule of solvation to give a two dimensional sheet (Figure 2.9).

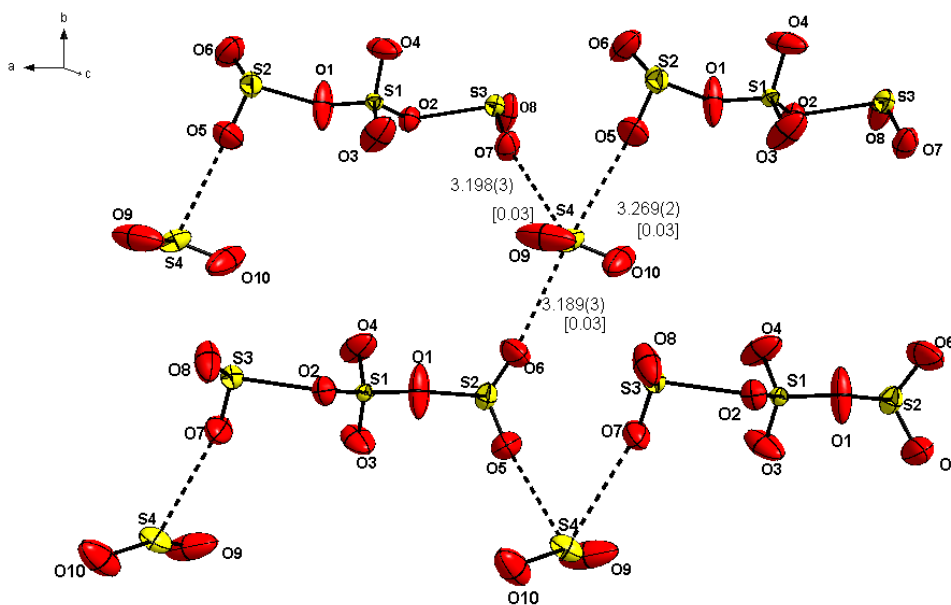


Figure 2.9. A portion of the layer of [(O₂SO)₂SO₂]²⁻ anion and weakly interacting SO₂ molecules of solvation in ab plane, bond distances (Å) and [bond orders]ⁱ (thermal ellipsoid plots are drawn at the 50% probability level).

The cations reside in between the layers formed by the anions and solvent molecules (Figure S.16). The anion and cations are linked by numerous O-H hydrogen bonds (Table S.7). The geometry of N(CH₃)₄⁺ is very similar to that in [N(CH₃)₄]₂SO₄ (Table S.8).⁸ The S-O distances in the SO₂ solvent molecule (S4-O10 1.394(4) Å, S4-O9 1.344(4) Å <SOS 120.022(2)) in [N(CH₃)₄]₂(O₂SO)₂SO₂•SO₂(s) are shorter than in SO₂(s)²¹ (1.4297(7), <SOS 117.5(1)) (Table S.6). Many X-ray structures containing SO₂ fragments

give S-O distances that are much shorter than expected^{17,18}, likely because of unresolved SO₂ disorder and/or unaccounted for librational motion.

2.2.3.G. The Structure and Bonding for [(O₂SO)₂SO₂]²⁻.

The experimental and calculated structures are in approximate agreement with some differences (Figure 2.7). This could be due to unaccounted disorder and/or librational motion in the SO₂ groups in the X-ray structure determination, the effect of O---H cation anion interactions, the influence of the interactions with the SO₂ solvate molecule or the limitations of the calculations at the (B3PW91/6-311+G(3df) level of theory. Two minimum conformations with almost the same energy (energy difference 2.3 kJ mol⁻¹) were optimized for [(O₂SO)₂SO₂]²⁻. The conformation that more resembled the experimental structure is presented in Figure 2.7. The large negative charges on the oxygen atoms in the anion are consistent with significant hydrogen bonding and anion distortion from the equilibrium gas phase geometry, especially that of the weak long S-O bridging bonds. The two SO₂ fragments in (O₂SO)₂SO₂²⁻ have different experimental geometries, possibly because of differing O—H anion cation interactions, and/or because of the different interactions with the SO₂ molecule of solvation. However the identity and overall structure of the dianion is not in doubt. It can be viewed as being formed by donation of electrons from the SO₄²⁻ to two SO₂ molecules resulting in a calculated charge of ca. -1.07 on the central SO₄ and ca. -0.46 on the terminal SO₂ groups. In valence bond terms the resulting calculated anion structure can be represented by resonance structures A and A' (Figure 2.10) with a calculated O-SO₂ bond order of ca. 0.5. The X-ray structure gives longer bridging sulfur-oxygen bonds S2-O1 (2.213(3) Å, B.O: 0.31)ⁱ S3-O2 (2.358(2) Å, B.O: 0.22)ⁱ than calculated 2.024 (B.O: 0.47)ⁱ implying

there is some contribution from the valence bond structure **B** in addition to **A** and **A'**. An even longer bridging O-SO₂ bond distance of 2.433(4) (B.O = 0.18)ⁱ was found in $[(\eta^6\text{-C}_6\text{H}_6)_2\text{Cr}]\text{S}_2\text{O}_6 \cdot 2\text{SO}_2$, formulated as an SO₂ solvate by the authors but which can also be viewed as a sulfur oxyanion S₄O₁₀²⁻ with an even greater contribution to bonding by a non-bonding resonance structure analogous to structure **B** in Figure 2.10.²³

Approximately 8000 S-O bond distances in the region 1.0 - 1.70 Å were found in the Cambridge Crystallographic Data Centreⁱⁱⁱ with approximately 600 in the range 1.70 – 2.00 Å and less than 50 in the range 2.00 – 2.50 Å, ie. sum of the Van der Waals radii of S and O is 3.32 Å.²⁴ The previously known very long S-O bonds (Figure S.14) can be regarded as part of a bond/no bond resonance system, or alternatively as part of a multicentred σ bond, eg. in the work by Martin et al.²⁵

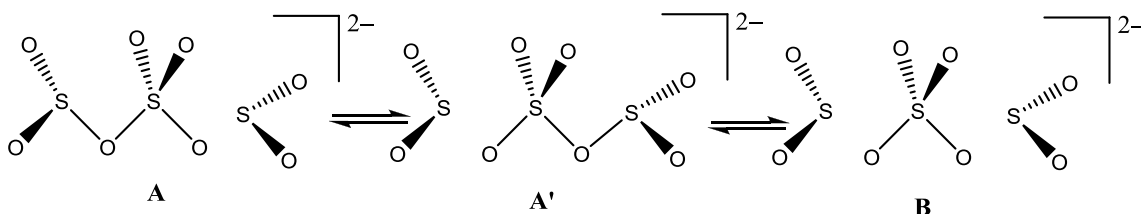


Figure 2.10. Valence bond description of $[(\text{O}_2\text{SO})_2\text{SO}_2]^{2-}$.

2.4. Conclusions.

We have shown that the use of Born-Haber cycles and volume based thermodynamics with DFT enthalpies of the corresponding gas phase reactions correctly predicts that $[\text{N}(\text{CH}_3)_4]_2\text{SO}_4$ will react with SO₂ to give $[\text{N}(\text{CH}_3)_4]_2\text{O}_3\text{SOSO}_2$ and $[\text{N}(\text{CH}_3)_4]_2(\text{O}_2\text{SO})_2\text{SO}_2$. Subsequently $[\text{N}(\text{CH}_3)_4]_2\text{SO}_4$ was experimentally shown to reversibly and quantitatively take up gaseous SO₂ at room temperature to produce

ⁱⁱⁱ Data obtained in August 2011.

$[\text{N}(\text{CH}_3)_4]_2\text{O}_3\text{SOSO}_2$, an isomer of the known $[\text{O}_3\text{SSO}_3]^{2-}$ dianion. This salt was unambiguously characterized using vibrational spectroscopy. Crystals of $[\text{N}(\text{CH}_3)_4]_2(\text{O}_2\text{SO})_2\text{SO}_2 \cdot \text{SO}_2$ were isolated from solutions of $[\text{N}(\text{CH}_3)_4]_2\text{SO}_4$ in liquid SO_2 . The X-ray structure showed that it contained the $[(\text{O}_2\text{SO})_2\text{SO}_2]^{2-}$ dianion. The $[\text{O}_3\text{SOSO}_2]^{2-}$ and $[(\text{O}_2\text{SO})_2\text{SO}_2]^{2-}$ oxyanions are the first new sulfur oxyanions containing 1 - 3 sulfur atoms that have been identified since 1891 (Table 1.1) and are the first members of a new class of $[\text{SO}_4][\text{SO}_2]_x^{2-}$ ($x = 1, 2$) sulfur oxyanions, analogous to the well known series of $\text{SO}_4[\text{SO}_3]_x^{2-}$ polysulfates (Table 1.1) isolated as salts of small cations.

This work illustrates the usefulness of predictive thermodynamics and the importance of size in salt reactivity. It implies that the chemistry of oxydianions of sulfur with large cations will be very different from that of the more traditional salts of small cations. This will be further illustrated in upcoming publications.²⁶ It also implies that the energetics of SO_2 uptake by sulfates can be tailored by changing the size of the cation. This represents a unique opportunity for the engineering of reversible SO_2 uptake reagents.

The present work compliments the classical 1938 studies by Jander and Mesech on the SO_2 uptake by $[\text{N}(\text{CH}_3)_4]_2\text{SO}_4$, and confirms their suggestion that $[\text{N}(\text{CH}_3)_4]_2 \cdot \text{SO}_4(\text{SO}_2)_x$ $x = 1$ and 2 were not just SO_2 solvates of $[\text{N}(\text{CH}_3)_4]_2\text{SO}_4$.

References

1. Greenwood, N. N.; Earnshaw, A. *Chemistry of the Elements*, 2nd ed., Pergamon Press: Oxford, UK, 1997.
2. Hill, J.C. *J. Chem. Educ.* 1979, *56*, 593.
3. Grein, F and Chan, J., *Computational & Theoretical Chemistry*, 2011, 966, 225.
4. Jansen, M.; Schatte, G.; Tobias, K. M.; Willner, H., *Inorg. Chem.*, **1988**, *27*, 1703.
5. Jander, G. and Mesech, H. *Z. physic. Chem.* 1938, *A183*, 121.
6. Pandey, R.; Biswas, R.; Chakrabarti, T.; Devotta, S. *Critical Reviews in Environmental Science and Technology* 2005, *35*, 571.
7. (a) Murchie, M.; Passmore, J. *Inorg. Synth.* 1990, *27*, 332. (b) Murchie, M. P.; Kapoor, R.; Passmore, J.; Schatte, G.; Way, T. *Inorg. Synth.* 1997, *31*, 102.
8. Malchus, M.; Jansen, M. *Acta Cryst.* **1998**, *B54*, 494.
9. CELL_NOW, V. 2008/2, George Sheldrick, Bruker AXS, Inc., Madison, Wisconsin, USA.
10. SAINT 7.23A, 2006, Bruker AXS, Inc., Madison, Wisconsin, USA.
11. TWINABS 1.05, George Sheldrick, 2004, Bruker Nonius, Inc., Madison, Wisconsin, USA.
12. Sheldrick, G.M. (2008). SHELXTL. *Acta Cryst.* *A64*, 112-122.
13. Frisch, M. J.; Trucks, G. W.; Schlegel, H. B.; Scuseria, G. E.; Robb, M. A.; Cheeseman, J. R.; Montgomery, Jr., J. A.; Vreven, T.; Kudin, K. N.; Burant, J. C.; Millam, J. M.; Iyengar, S. S.; Tomasi, J.; Barone, V.; Mennucci, B.; Cossi,

M.; Scalmani, G.; Rega, N.; Petersson, G. A.; Nakatsuji, H.; Hada, M.; Ehara, M.; Toyota, K.; Fukuda, R.; Hasegawa, J.; Ishida, M.; Nakajima, T.; Honda, Y.; Kitao, O.; Nakai, H.; Klene, M.; Li, X.; Knox, J. E.; Hratchian, H. P.; Cross, J. B.; Bakken, V.; Adamo, C.; Jaramillo, J.; Gomperts, R.; Stratmann, R. E.; Yazyev, O.; Austin, A. J.; Cammi, R.; Pomelli, C.; Ochterski, J. W.; Ayala, P. Y.; Morokuma, K.; Voth, G. A.; Salvador, P.; Dannenberg, J. J.; Zakrzewski, V. G.; Dapprich, S.; Daniels, A. D.; Strain, M. C.; Farkas, O.; Malick, D. K.; Rabuck, A. D.; Raghavachari, K.; Foresman, J. B.; Ortiz, J. V.; Cui, Q.; Baboul, A. G.; Clifford, S.; Cioslowski, J.; Stefanov, B. B.; Liu, G.; Liashenko, A.; Piskorz, P.; Komaromi, I.; Martin, R. L.; Fox, D. J.; Keith, T.; Al-Laham, M. A.; Peng, C. Y.; Nanayakkara, A.; Challacombe, M.; Gill, P. M. W.; Johnson, B.; Chen, W.; Wong, M. W.; Gonzalez, C.; and Pople, J. A.; *Gaussian 03*, revision E.01, Gaussian, Inc., Wallingford CT, 2004.

14. (a) Becke, A. D. *J. Chem. Phys.* **1993**, *98*, 5648. (b) Perdew, J. P.; Wang, Y. *Phys. Rev. B* **1992**, *45*, 13244.
15. Raghavachari, K.; Binkley, J. S.; Seeger, R.; Pople, J. A., *J. Chem. Phys.*, **1980**, *72*, 650.
16. Zhurko, G. A.; Zhurko, D. A. ChemCraft Version 1.6 (Build 350), Tool for Treatment of the Chemical Data.
17. Decken, A.; Knapp, C. Nikiforov, G. B.; Passmore, J.; Rautiainen, J. M.; Wang, X., Zeng, X. *Chem. J. Eur.* **2009**, *15*, 6504 and references within.
18. Kumar, A.; McGrady, G. S.; Passmore, J.; Grein, F.; Decken, A. *Z. Anorg. Allg. Chem.* **2012**, *638*, 744 and references within.

19. Degen, I.A.; Newman, G.A. *Spectrochimica Acta*, **1993**, 49A, 859. and Palmer, W.G. *J. Chem. Soc.*, **1961**, 1552.
20. Risberg, E.D.; Eriksson, L.; Mink, J.; Pettersson, L.G.M.; Skripkin, M.Y.; Sandström, M. *Inorganic Chemistry*, 2007, 46, 8332.
21. Anderson, A.; Savoie, R. *Canadian Journal of Chemistry* 1965, 43, 2271.
22. Steudel, R.; Steudel, Y. *Eur. J. Inorg. Chem.* 2009, 1393.
23. Elschenbroich, C.; Gondrum, R.; Massa, W. *Angewandte Chemie*, **1985**, 97, 976.
24. Bondi, A. *J. Phys. Chem.*, **1964**, 68, 441.
25. (a) Perkins, C.W.; Wilson, S.R.; Martin, J.C. *J. Am. Chem. Soc.*, 107, **1985**, 3209. (b) Lam, W.Y.; Duesler, E.N.; Martin, J.C. *J. Am. Chem. Soc.*, 103, **1981**, 127.
26. Passmore, J. et al. *Inorganic Chemistry* To be published.

Chapter 3. Conclusions and Future Work.

The two main goals (1) the absorption and release of SO₂ using a sulfur oxydianion and (2) preparation and characterization of two novel sulfur oxydianions was accomplished.

Goal (1) Conclusions:

- We predicted that SO₂ would react with SO₄²⁻ salts of large cations under ambient conditions, and this was shown to be the case. [N(CH₃)₄]₂SO₄ reacts with SO₂ under mild conditions.
- The process was reversible under mild conditions and of potential interest in an industrial context. However, the products and reactants react readily with water. The products also released the SO₂ slowly over time if not contained in a sealed tube.

Goal (2) Conclusions:

- This work demonstrates the usefulness of volume based thermodynamics for predicting the synthesis of new classes of simple binary anions of the elements.
- One mole equivalent of SO₂ reacts with [N(CH₃)₄]₂SO₄(s) to give [N(CH₃)₄]₂O₃SOSO₂(s) containing the new [O₃SOSO₂]²⁻ anion which is an isomer of the known dithionate, [O₃SSO₃]²⁻. The vibrational spectra of this are in excellent agreement with the calculated frequencies (B3PW91/6-311+G(3df)).
- The addition of two mole equivalents of SO₂ to [N(CH₃)₄]₂SO₄ leads to a mixture which was characterized by Raman spectroscopy and shown to contain another new sulfur oxyanion, [(O₂SO)₂SO₂]²⁻. Crystals of [N(CH₃)₄]₂(O₂SO)₂SO₂•SO₂

were isolated from solutions of $[\text{N}(\text{CH}_3)_4]_2\text{SO}_4$ in liquid SO_2 and contained the $[(\text{O}_2\text{SO})_2\text{SO}_2]^{2-}$ dianion, which was characterized by X-ray crystallography.

- The addition of the weak Lewis acid SO_2 ($x = 1$ and 2) to $[\text{N}(\text{CH}_3)_4]_2\text{SO}_4$ presents a new class of sulfur oxydianions. The new series is similar to the polysulfates which are obtained in the addition of the strong Lewis acid SO_3 to R_2SO_4 salts where R can be a small counteraction.
- The known sulfur oxydianions previous to this work have been known for over a century as seen in Table 1.1.
- This work presents the preparation and characterization of two new sulfur oxydianions ($[\text{O}_3\text{SOSO}_2]^{2-}$ and $[(\text{O}_2\text{SO})_2\text{SO}_2]^{2-}$) and other group members have also obtained $(\text{SO}_2)_3^{2-}$, $\text{S}_4\text{O}_4^{2-}$ and 3 uncharacterized compounds. The Passmore group has significantly increased the number of sulfur oxydianions and these findings re-open sulfur oxydianion chemistry as shown in Table 3.1.

Table 3.1. New and Known Sulfur Oxydianions Containing 1 - 5 Sulfur Atoms in the Solid State.

Increasing Number of Sulfur Atoms →				
1	2	3	4	5
[SO ₃] ²⁻ 1702 Stahl [2K ⁺]	[O ₃ S-S] ²⁻ 1799 Chaussie [2Na ⁺]		[O ₃ S-S-S-SO ₃] 1848 Kessler [2Na ⁺]	[O ₃ S-S-S-S-S-O ₃] 1882 Lenoir [2K ⁺]
	[O ₂ S-SO ₂] ²⁻ 1825 Berzelius [2Na ⁺]	[SO ₂] ₃ ²⁻ 2011 Greer [N(CH ₃) ₄] ⁺ /[N(C ₂ H ₅) ⁺] 2011 Paulose [Me ₂ N] ₂ CC(NMe ₂) ₂ ²⁺	[O ₂ S-S-S-SO ₂] ²⁻ 2011 Paulose [Me ₂ N] ₂ CC[NMe ₂] ₂ ²⁺ + 3 Uncharacterized compounds containing the [Me ₂ N] ₂ CC[NMe ₂] ₂ ²⁺ countercation	
	[O ₃ S-SO ₂] ²⁻ 1797 Vauquelin [2Na ⁺]			
	[O ₃ S-SO ₃] ²⁻ 1819 Gay- Lussac [Mn ²⁺]	[O ₃ S-S-SO ₃] ²⁻ 1841 Langlois [2K ⁺]		
	[O ₃ S-O-SO ₂] ²⁻ 2011 Richardson [N(CH ₃) ₄] ⁺	[O ₂ S-O ₃ S-O-SO ₂] ²⁻ 2011 Richardson [N(CH ₃) ₄] ⁺		
[SO ₄] ²⁻ 1625 Glauber [2Na ⁺]	[O ₃ S-O-SO ₃] ²⁻ 1861 Rosenstiehl [2Na ⁺ /2K ⁺]	[O ₃ SOSO ₂ OSO ₃] ²⁻ 1868 Schultz-Sellack [2Na ⁺]	[O ₃ SO-(SO ₂)-O- (SO ₂)-O-SO ₃] 2012 Wickleder ¹ [NO ₂] ²⁺	[O ₃ SO-(SO ₂)- O-(SO ₂)-O- (SO ₂)-OSO ₃] 1884 Weber [2K ⁺]
	[O ₃ S-O-O- SO ₃] ²⁻ 1891 Marshall [2K ⁺]			

* Oxydianion; Year Discoverer [Counter Cation]²

Future Work

- The preparation of salts of SO₄²⁻ of larger counter cations (ie. N(C₂H₅)₄⁺) to capture SO₂ should be examined since the absorption of SO₂ has been predicted to be more favourable to larger salts (Figure 2.2). Larger cationic sulfate salt preparations are available but the purity of these salts is questionable. Quaternary tetraalkylammonium salts can be prepared most commonly by metathesis reactions:^{3,4,5,6,7,8} Tetraalkylammonium sulfates are not always easily attainable

using these routes because of the aqueous environments that prompt decomposition and/or challenging separation of products from a mixture produced by metathesis reactions. However, preparation of the larger cationic sulfates does seem feasible. My preliminary results suggest that tetraethylammonium sulfate can be prepared using an ion exchange method, but current product did contain some impurities.

- The thermodynamics of the system need to be established from vapour pressure measurements of $[\text{N}(\text{CH}_3)_4]_2\text{O}_3\text{SOSO}_2$ as a function of temperature and improved constants in the V.B.T expression for the lattice energy obtained. The improved expressions for the V.B.T enthalpy can then be obtained thus enabling more accurate predictions of the reactivity of the tetralkylammonium sulfates.
- To determine if smaller cationic salts can stabilize these new sulfur oxyanions, a reaction at low temperature for the addition of liquid SO_2 to small cationic sulfates such as Cs_2SO_4 should be investigated.
- $[\text{N}(\text{CH}_3)_4]_2\text{SO}_4$ and other sulfur oxydianion salts react with water and oxygen (two components in flue gases) and are therefore unlikely compounds for SO_2 uptake in industry. However, simulating an industrial capture of SO_2 using tetramethylammonium sulfate and determining if SO_2 is still captured under a stream of flow flue gases would be of interest. The process could be tested by removing the oxygen and water from the flue gas first and allowing the remainder of the gases through to determine if the capture of SO_2 is still effective.

- V.B.T, Born Haber cycle and gas phase data predict that tetramethylammonium sulfate will capture CO₂ to obtain [N(CH₃)₄]₂O₃SOCO₂. Reactions of R₂SO₄ (eg R = N(CH₃)₄⁺) with CO₂ should be investigated.
- Analogous reactions using salts of SeO₄²⁻ instead of SO₄²⁻ for the uptake of selenium dioxide should be examined theoretically and experimentally.
- The addition of sulfur to salts of SO₄²⁻ (Eq. 3.1) should be examined if thermodynamically feasible. Sulfur has been added to salts containing the sulfite anion to form the known thiosulfate compound (Eq. 3.2).⁹



R₂SOSO₃ may be observed rather than the known [O₂SSO₂]²⁻. If not and the [O₂SSO₂]²⁻ salt is formed, it provides a new route to prepare dithionites with large cations. The [SOSO₃]²⁻ structure has been calculated to be the more stable in the gas phase.¹⁰

References

1. Logemann, C.; Klüner, T.; Wickleder, M.S. *Angew. Chem. Int. Ed.* **2012**, *51*, 4997.
2. Mellor, J.W. *A Comprehensive Treatise on Inorganic and Theoretical Chemistry*, Vol. X, Logmans Green and Co. LTD.: London, UK, 1940 and references within.
3. Malchus, M.; Jansen, M. *Acta Cryst.* **1998**, *B54*, 494.
4. Markowitz, M.M *Journal of Organic Chemistry* **1957**, *22*, 983.
5. Leftin, H.P.; Lichtin, N.N. *J. Am. Chem. Soc.* **1957**, *79*, 2475.
6. McLean, W.J.; Jeffrey, G.A. *J. Chem. Phys.* **1968**, *49*, 4556.
7. Lam, Y.S.; Mal, T.C.W. *Journal of Applied Crystallography* **1978**, *11*, 193.
8. Husain, M.M.; Singh, D.K. *Synth. React, Inorg. Met.-org. Chem.* **1984**, *14*, 49.
9. Blitz, H. *Laboratory Methods of Inorganic Chemistry*, J. Wiley & Sons: New York, NY, 1909.
10. Steudel, R.; Steiger, T. *Journal of Molecular Structure (Theochem)* **1993**, *284*, 55.

Supporting Information

S.1. Thermodynamics.

S.1.A. Volume Based Thermodynamics (V.B.T). The V.B.T lattice potential of a solid is given by equation S.1.¹

$$U_{\text{pot}} = |z_+| |z_-| v \left(\frac{\alpha}{V^{1/3}} + \beta \right) \quad (\text{S.1})$$

Where z_+ = charge of cation, z_- = charge on anion, v = total number of ions per molecular unit ($p + q$), α and β = coefficients (165.3 kJ/mol and -29.8 kJ/mol for a 2:1 salt respectively), V = volume of a molecular unit in the salt

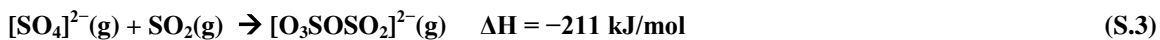
The V.B.T lattice enthalpy of a solid is given by equation S.2.^{1,2}

$$\Delta H = U_{\text{pot}}(M_p X_q) + \left[\left(\frac{p n_M}{2} - 2 \right) + \left(\frac{q n_X}{2} - 2 \right) \right] RT \quad (\text{S.2})$$

Where p = number of cations, q = number of anions, n_M and n_X = 6 for polyatomic nonlinear ions, R = gas constant, T = temperature

Materials with the greatest potential for the sequestration of SO_2 are M_2X salts which incorporate large, kinetically stable cations such as the tetraalkylammonium cations. Our synthetic protocol is based on employing large cations as the starting material, thus taking advantage of the inverse cube root relationship and minimizing the unfavourable lattice enthalpy change in the overall reaction. A smaller value change of the lattice enthalpy in the solid state will directly affect the overall enthalpy of reaction and result in a more

favorable process. The calculated gas phase enthalpies of equations **S.3**, **S.4** and **S.5** have previously been reported by one of us (Grein).



Using an appropriate Born-Haber cycle (eg. Figure 2.1 for $\text{R}_2\text{SO}_4(\text{s})$) along with lattice enthalpies, derived from V.B.T, and calculated gas phase enthalpies (B3PW91-6-311+G(3df)) the favorability of an $\text{SO}_2(\text{g})$ uptake reaction is estimated. The Gibbs free energy (ΔG) (Table S.2) of the reaction for various R in equation **S.6** is given by equation **S.7**.



$$\Delta\text{G} = \Delta\text{H} - T\Delta\text{S} \text{ at } 298 \text{ K} \quad (\text{S.7})$$

where ΔH is the enthalpy of reaction derived from the Born-Haber cycle, T is the temperature (298 K) and ΔS is the entropy. The changes in the Gibbs energy of reactions versus cation volume for the sulfate system were then graphed (Figure 2.2, for uptake of 1 and 2 moles of $\text{SO}_2(\text{g})$).

Table S.1. Estimation of the Gibbs free energy (298 K) for the uptake of SO₂(g) by R₂SO₄(s).

R ^{+a}	$\Delta H_{\text{lattice}}^b$ (298 K) (kJ/mol)		$\Delta H_{\text{lattice}}$ (298 K) (kJ/mol)				ΔH_{rxn} (298 K) (kJ/mol)	ΔG_{rxn} (298 K) ^c (kJ/mol)
R₂SO₄(s) + SO₂(g) → R₂O₃SOSO₂(s) (S.8)								
	R ₂ SO ₄ (s)	R ₂ O ₃ SOSO ₂ (s)	R ₂ (O ₂ SO) ₂ SO ₂ (s)	R ₂ O ₃ SOSO ₂ (s)	R ₂ (O ₂ SO) ₂ SO ₂ (s)	R ₂ S ₄ O ₁₀ (s)		
2(Na ⁺) (V = 0.008 nm ³)	1966			1671			85	136
2(Cs ⁺) (V = 0.038 nm ³)	1784			1564			9	61
2[N(CH ₃) ₄] ⁺ (V = 0.226 nm ³)	1276			1200			-135	-84
2[N(CH ₃ CH ₂) ₄] ⁺ (V = 0.398 nm ³)	1081			1036			-167	-115
2[N(CH ₃ CH ₂ CH ₂ CH ₂) ₄] ⁺ (V = 0.826 nm ³)	842			822			-191	-140
R₂O₃SOSO₂(s) + SO₂(g) → R₂(O₂SO)₂SO₂(s) (S.9)								
2(Na ⁺) (V = 0.008 nm ³)		1671			1491		61	112
2(Cs ⁺) (V = 0.038 nm ³)		1564			1418		27	79
2[N(CH ₃) ₄] ⁺ (V = 0.226 nm ³)		1200			1138		-57	-5
2[N(CH ₃ CH ₂) ₄] ⁺ (V = 0.398 nm ³)		1036			997		-80	-29
2[N(CH ₃ CH ₂ CH ₂ CH ₂) ₄] ⁺ (V = 0.826 nm ³)		822			804		-101	-49
R₂(O₂SO)₂SO₂(s) + SO₂(g) → R₂(O₂SO)₂(SO₂)(s) (S.10)								
2(Na ⁺) (V = 0.008 nm ³)			1491			1366	67	118
2(Cs ⁺) (V = 0.038 nm ³)			1418			1311	48	99
2[N(CH ₃) ₄] ⁺ (V = 0.226 nm ³)			1138			1085	-6	49
2[N(CH ₃ CH ₂) ₄] ⁺ (V = 0.398 nm ³)			997			963	-25	27
2[N(CH ₃ CH ₂ CH ₂ CH ₂) ₄] ⁺ (V = 0.806 nm ³)			804			787	-42	10

^a Volumes of Na⁺, Cs⁺, [N(CH₃)₄]⁺, [N(CH₃CH₂)₄]⁺ and [N(CH₃CH₂CH₂CH₂)₄]⁺ obtained in Reference 1.
Volume of [N(CH₃CH₂CH₂CH₂)₄]⁺ obtained from an average of crystal structures in References 3,4,5 and 6.

$$\begin{aligned} \text{Vol SO}_4^{2-} &= \text{Vol (molecular unit) [N(CH}_3)_4\text{]}_2\text{SO}_4^7 - \text{Vol N(CH}_3)_4^{+1} \\ &= 0.32015 \text{ nm}^3 - 0.113 \text{ nm}^3 \\ &= 0.094 \text{ nm}^3 \text{ (Volume of SO}_4^{2-} \text{ reported in literature, } 0.091 \pm 0.013 \text{ nm}^3)^1 \end{aligned}$$

$$\begin{aligned} \text{Vol [O}_3\text{SOSO}_2\text{]}^{2-} &= \text{Vol SO}_4^{2-} + \text{Vol SO}_2(\text{s})^8 \\ &= 0.094 \text{ nm}^3 + 0.055 \text{ nm}^3 \\ &= 0.149 \text{ nm}^3 \text{ (Volume of [O}_3\text{SSO}_3\text{]}^{2-} \text{ isomer reported in literature, } 0.153 \pm 0.014 \text{ nm}^3)^1 \end{aligned}$$

$$\begin{aligned} \text{Vol [(O}_2\text{SO)}_2\text{SO}_2^{2-}] &= \text{Vol SO}_4^{2-} + \text{Vol 2 x SO}_2(\text{s})^8 \\ &= 0.094 \text{ nm}^3 + (2 \times 0.055 \text{ nm}^3) \\ &= 0.204 \text{ nm}^3 \end{aligned}$$

$$\begin{aligned} \text{Vol [S}_4\text{O}_{10}\text{]}^{2-} &= \text{Vol SO}_4^{2-} + \text{Vol 3 x SO}_2(\text{s})^8 \\ &= 0.094 \text{ nm}^3 + (3 \times 0.055 \text{ nm}^3) \\ &= 0.259 \text{ nm}^3 \end{aligned}$$

Note the small changes in volume of the molecular unit lead to minimal changes in the corresponding U_{pot} as this is proportional to 1/V^{1/3}.²

^c where $\Delta G_{\text{rxn}} (298 \text{ K}) = \Delta H_{\text{rxn}} - T\Delta S$.

The entropy for the solid phase is calculated from Jenkins et al. equation **S.11**:²

$$\Delta S = k(\Delta V) \tag{S.11}$$

where k = 1360 J/molK and ΔV is the difference in volumes equal to the value of 1 SO₂ (0.055 nm³) therefore ΔS_{solid} (SO₂) = 0.0748 kJ/molK. The entropy for the gas phase obtained from NIST is ΔS_{gas} (SO₂) = 0.2481 kJ/molK. Therefore ΔS(SO₂) = 0.1733 kJ/molK and -TΔS (298 K) = 51.5 kJ/mol.

S2. Experimental

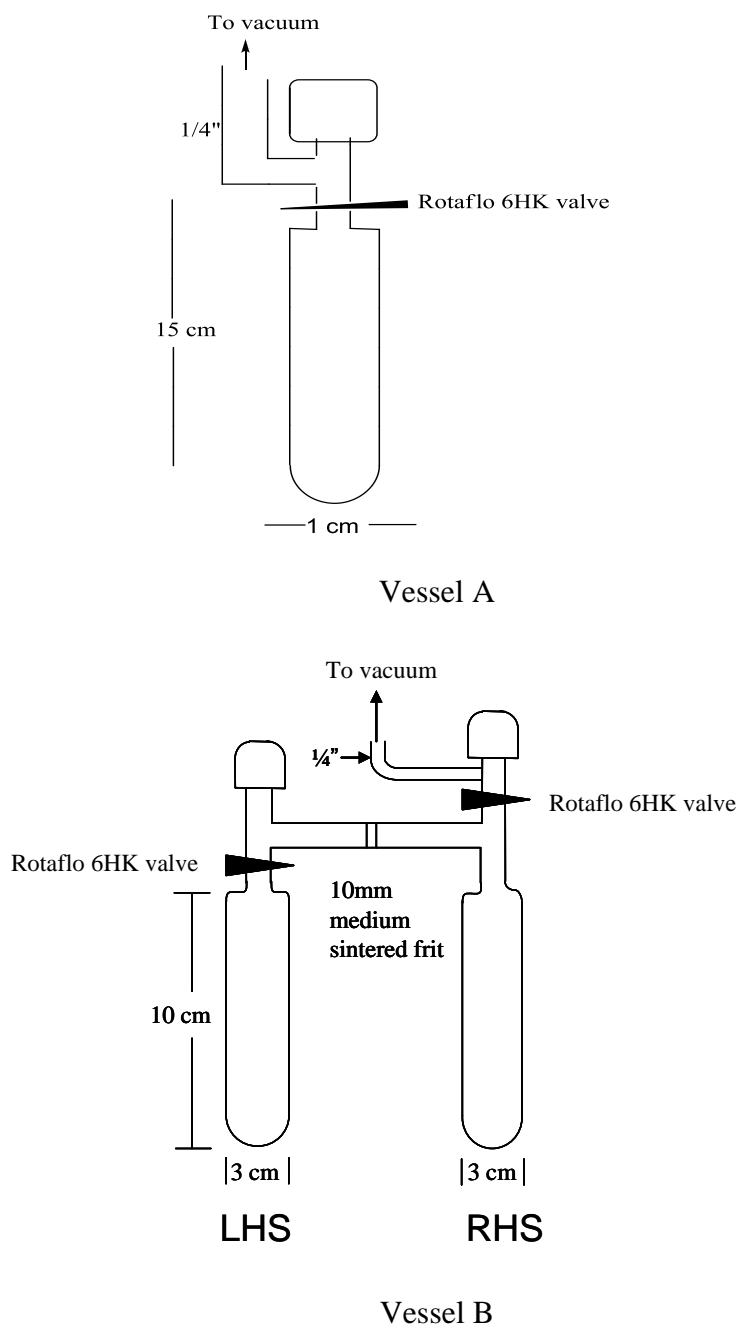


Figure S.1. Illustration of vessels A and B.

S.2.1. An *in situ* Preparation of $[\text{N}(\text{CH}_3)_4]_2\text{O}_3\text{SOSO}_2(\text{s})$. 0.970 g of $[\text{N}(\text{CH}_3)_4]_2\text{SO}_4(\text{s})$ (0.970 g, 3.970 mmol), white free flowing powder, was added to carefully flame dried vessel A, using a loader and scupula. One mole equivalent of $\text{SO}_2(\text{g})$ (0.256 g, 4.000 mmol) according to equation 2.4 ($\text{R} = \text{N}(\text{CH}_3)_4^+$) was expanded into the line and then into vessel A. The white free flowing powder immediately became partly clumped and yellowish in color. The vapour pressure dropped from 1400.0 mm Hg to 95.0 ± 2.5 mm Hg in approximately 4 hours at which time there was change of only ± 2.5 mm Hg over a half hour period in vapour pressure (95.0 mm Hg). The remaining $\text{SO}_2(\text{g})$ in the line was condensed into, and isolated in, vessel A. The vessel was weighed and then partly submerged into a sonicating bath at RT (20 °C) for 20 minute periods as well as shaken by hand in order to obtain a homogeneous sample. After approximately 1 - 2 hours, the compound turned completely white and free flowing. The yellow color initially seen when $\text{SO}_2(\text{g})$ was introduced to the sample was not observed again. *In situ* Raman spectra were obtained approximately every 8 - 12 hours over a 7 day period and a summary of the spectra with assignments are given in Figure S.3 and Table S.2 (product weight = 1.226 g). The IR spectrum of the product is given in Figure S.4 and S.5 with assignments and compared with that of $[\text{N}(\text{CH}_3)_4]_2\text{SO}_4$ and calculated IR of $[\text{O}_3\text{SOSO}_2]^{2-}$. The vibrational assignments are given in Table S.2, with assignments for the anion made by comparison with the calculated spectrum of $[\text{O}_3\text{SOSO}_2]^{2-}$. It was found that if the $\text{SO}_2(\text{g})$ was expanded into the line and not confined in the vessel for the full seven days SO_2 of solvation and other species were always observed in Raman spectra. The vapour pressure of products from repeated reactions ranged from 5 - 11 mm Hg, using $[\text{N}(\text{CH}_3)_4]_2\text{SO}_4$ from Aldrich and TCI. The vapour pressure of the product using spectroscopically pure

$[\text{N}(\text{CH}_3)_4]_2\text{SO}_4$ obtained from Aldrich was 11.0 mm of Hg after 7 days with a Raman spectrum identical to that given in Figure S.3. The sample from TCI gave the same results but the reaction went to completion in 1 day and was also a white free flowing powder. The addition of 0.85 mole equivalents also gave similar vapour pressure (7.0 mm Hg) measurements and Raman spectra but in addition with bands attributable to other species.

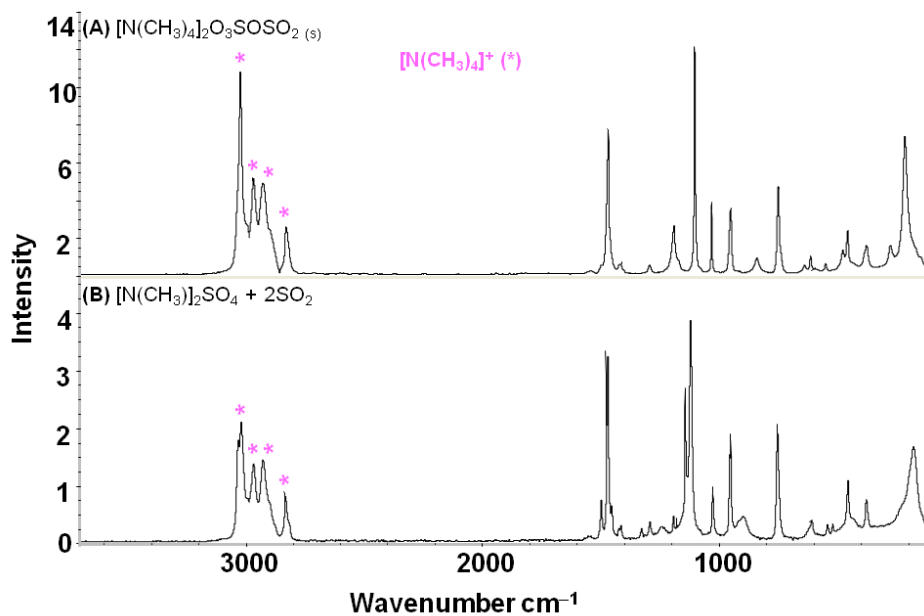


Figure S.2. Raman spectra of $[\text{N}(\text{CH}_3)_4]_2\text{O}_3\text{SOSO}_2$ (A) and $[\text{N}(\text{CH}_3)_4]_2\text{SO}_4 + 2\text{SO}_2$ (B) in 1400 - 4000 cm^{-1} region (Scans: 2048; Resolution: 4cm^{-1} ; Detector: Ge) with 0.205 W power.

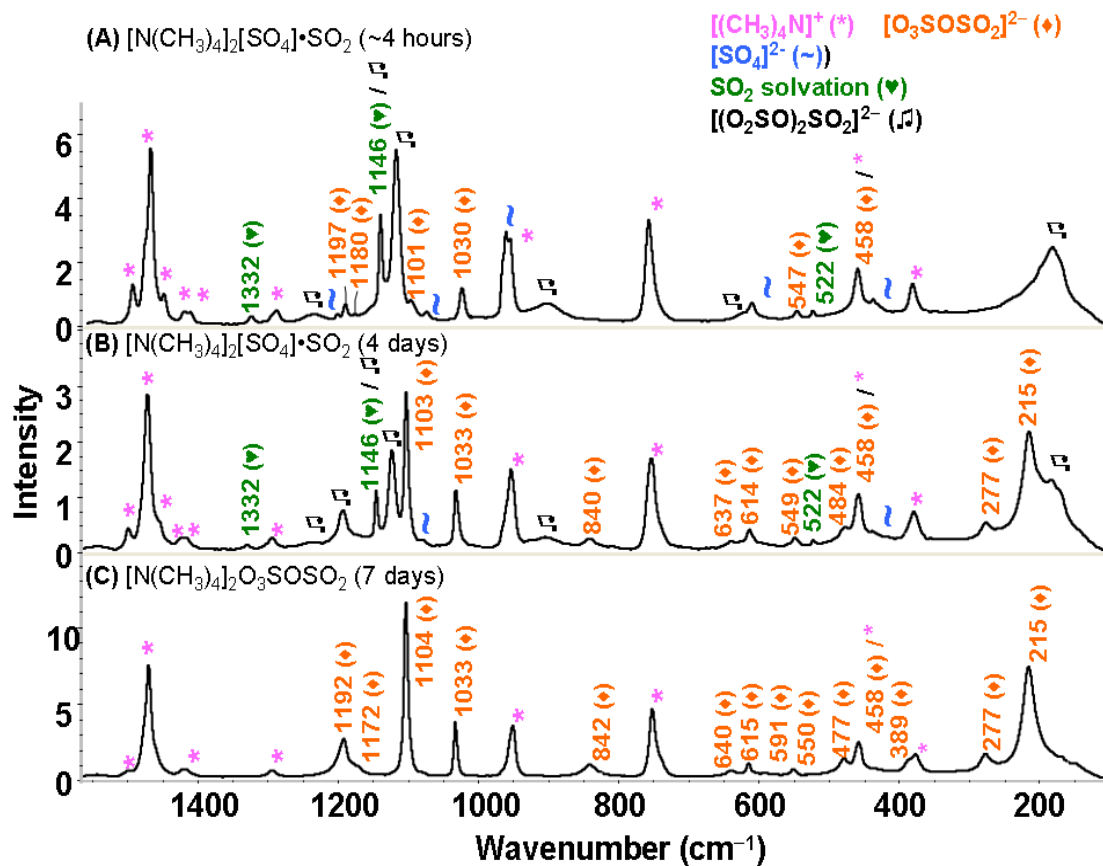


Figure S.3. Raman spectra of a 1:1 SO_2 : $[\text{N}(\text{CH}_3)_4]_2\text{SO}_4(\text{s})$ as a function of time in the 140 - 1500 cm^{-1} region. Scans: 2048; resolution: 4cm^{-1} ; laser power: 0.205 W where (A) (C) used a Ge detector and (B) used a InGaAs detector. Spectra of the 1500-3500 cm^{-1} region after 7 days included in Figure S.2. Assignments related to $\text{N}(\text{CH}_3)_4^+$ and SO_4^{2-} were made by comparison with those in $[\text{N}(\text{CH}_3)_4]_2\text{SO}_4(\text{s})$ ⁷ and SO_2 of solvation with similar compounds found in Table S.6.

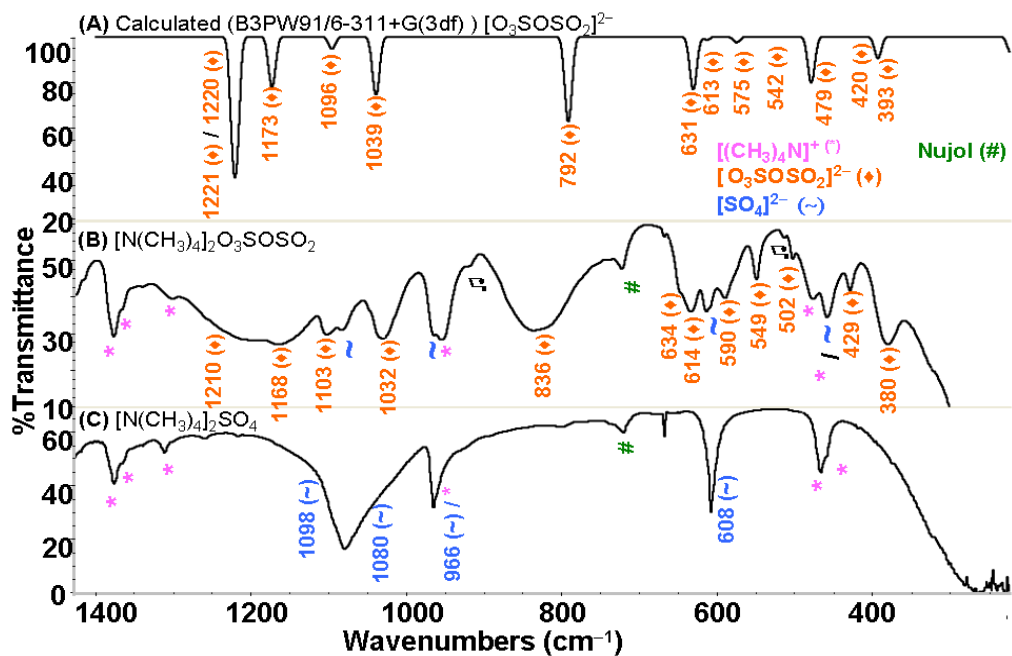


Figure S.4. Infrared spectra of [N(CH₃)₄]₂O₃SOSO₂(s) (scans: 32; Resolution: 4cm⁻¹) compared with starting material, [N(CH₃)₄]₂SO₄(s), and calculated spectra of [O₃SOSO₂]²⁻ in 140 - 1400 cm⁻¹ region. Spectra of the 1500-3500 cm⁻¹ region is given in S.5. Assignments related to N(CH₃)₄⁺ and SO₄²⁻ were made by comparison with those in [N(CH₃)₄]₂SO₄(s).⁷ There are also bands that are attributed to SO₄²⁻ that likely come from the loss of SO₂ from the [O₃SOSO₂]²⁻ on sample preparation.

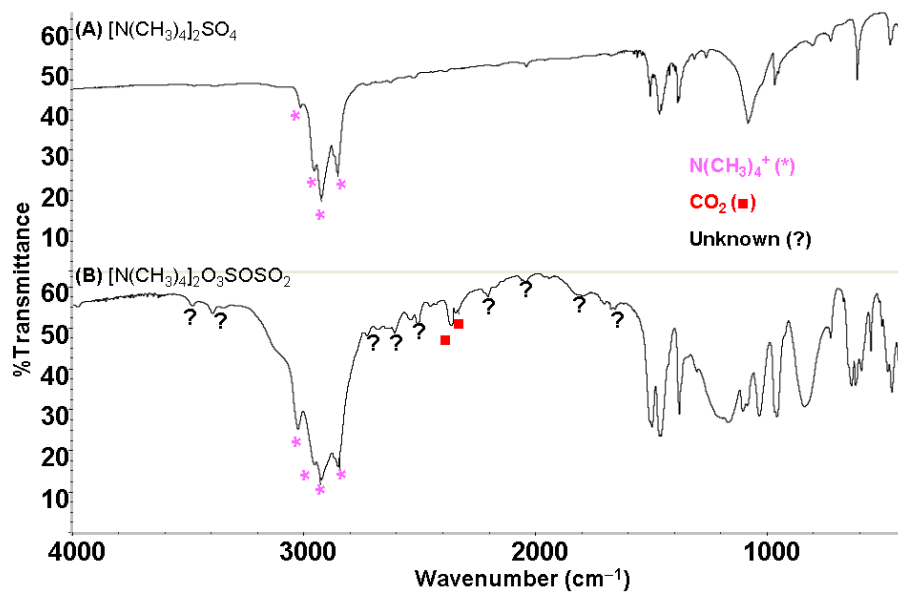


Figure S.5. Infrared spectra of [N(CH₃)₄]₂O₃SOSO₂ compared with that of the starting material, [N(CH₃)₄]₂SO₄, in 140 – 4000 cm⁻¹ region (scans: 32; Resolution: 4cm⁻¹).

Table S.2. The experimental vibrational spectrum (frequencies cm^{-1} , relative intensities in brackets) of $[\text{O}_3\text{SOSO}_2]^{2-}$ in $[\text{N}(\text{CH}_3)_4]_2\text{O}_3\text{SOSO}_2(\text{s})$, compared with the calculated (B3PW91/6-311+G(3df)) spectrum.

$[\text{N}(\text{CH}_3)_4]_2\text{O}_3\text{SOSO}_2(\text{s})$		Calculated [B3PW91/6-311+G(3df)] for $[\text{O}_3\text{SOSO}_2]^{2-}$		Assignment ^{a,b}
Raman	IR	Raman	IR	
		35 (1)	35 (<1)	$A'' [\text{O}_3\text{SOSO}_2]^{2-}$
		45 (<1)	45 (<1)	$A'' [\text{O}_3\text{SOSO}_2]^{2-}$
		132 (3)	132 (1)	$A' \nu(\text{O}_2\text{S-O})$
215 (84)		222 (42)	222 (13)	$A'' \rho(\text{SO}_2)$ $\rho(\text{SO}_3)$
277 (15)		279 (9)	279 (<1)	$\nu_8(\text{E})\delta\text{C}_4\text{N}$
378 (8)				$A' \rho(\text{SO}_2)$ $\rho(\text{SO}_3)$
389 (9)	380 (12)	393 (4)	393 (18)	$A'' \delta_{\text{as}}(\text{SO}_3)$ $\nu_{19}(\text{F}_2)\delta\text{C}_4\text{N}$ $\nu_{19}(\text{F}_2) \delta\text{C}_4\text{N}$ $A' \delta_{\text{s}}(\text{SO}_3)$ $\delta(\text{SO}_2)$
	429 (3)	420 (1)	420 (<1)	
458 (12)	458 (12)	--		
477 (10)	476 (9)	479 (17)	479 (40)	
	502 (2)			?
	514 (<1)			$A' \delta(\text{SO}_3)$ $\delta(\text{SO}_2)$
550 (3)	549 (5)	542 (10)	542 (1)	$A'' \rho_{\text{r}}(\text{SO}_3)$
591 (2)	590 (14)	575 (3)	575 (5)	$\nu_4(\text{F}_2) \delta_{\text{d}}\text{SO}_3$ $\delta_{\text{d}}\text{SO}_3$
	608 (15)			$A' \rho(\text{SO}_3)$ $\delta(\text{SO}_2)$ $\nu(\text{O}_2\text{S-O})$
615 (3)	614 (15)	613 (16)	613 (2)	$A' \nu(\text{O}_2\text{S-O})$ $\delta(\text{SOS})$ $\delta_{\text{as}}(\text{SO}_3)$
640 (3)	634 (21)	630 (8)	630 (48)	?
	649 (21)			Nujol
	721 (8)			$\nu_3(\text{A}_1) \nu_{\text{sym}}\text{C}_4\text{N}$ $\nu_{\text{s}}\text{C}_4\text{N}$
752 (22)				$A' \nu_{\text{s}}(\text{O}_3\text{S-O})$
842 (7)	836 (100)	792 (27)	792 (84)	?
	917 (<1)			$\nu_{18}(\text{F}_2)\nu_{\text{as}}\text{C}_4\text{N}$ $\nu_{\text{as}}\text{C}_4\text{N}$ $\nu_1(\text{A}_1)\nu_{\text{s}}\text{SO}_4$ $2\nu_{19}$
951 (15)	955 (22)			
	964 (19)			$A' \nu_{\text{s}}(\text{SO}_3)$ $\nu_{\text{s}}(\text{SO}_2)$
1033 (9)	1032 (47)	1039 (41)	1039 (53)	$\nu_3(\text{F}_2)\nu_{\text{d}}\text{SO}_3$

	1080 (26)			A' $\nu_s(\text{SO}_2)$ $\nu_s(\text{SO}_3)$
1104 (37)	1103 (23)	1096 (100)	1096 (10)	A'' $\nu_{as}(\text{SO}_2)$ $\nu_{as}(\text{SO}_3)$
1172 (3)	1168 (58)	1173 (47)	1173 (45)	A'' $\nu_{as}(\text{SO}_3)$
1192 (19)	1210 (87)	1221 (52)	1221 (76)	A' $\nu_{as}(\text{SO}_3)$ $\nu_{as}(\text{SO}_2)$
1192 (19)	1210 (87)	1222 (12)	1222 (100)	$\nu_{17}(\text{F}_2)\text{CH}_3$ rock
1294 (3)	1302 (19)			$\nu_{16}(\text{F}_2)\delta_{\text{sym}}\text{CH}_3$
1417 (4)				$\nu_6(\text{E})\delta_{as}\text{CH}_3$
1471 (39)	1462 (53)			$\nu_{15}(\text{F}_2)\delta_{as}\text{CH}_3$
1498 (3)	1496 (46)			$\nu_{13}(\text{F}_2)\nu_{as}\text{CH}_3$ $\nu_5(\text{E})\nu_{as}\text{CH}_3$ $\nu_{14}(\text{F}_2)\nu_{\text{sym}}\text{CH}_3$ $\nu_1(\text{A}_1)\nu_{\text{sym}}\text{CH}_3$ + combination bands +Nujol
2832 (21)	2853 (84)			
2929 (71)	2924 (70)			
2970 (52)				
3025 (100)	3031 (79)			

^aAssignment for $\text{N}(\text{CH}_3)_4^+$ as given for $[\text{N}(\text{CH}_3)_4]_2\text{SO}_4$.⁷

^bbands were assigned visually with the aid of ChemCraft; ν - stretching, δ - bending, ρ - twisting/rocking/wagging

Table S.3. Comparison of Cl₂O₆⁹, the calculated [O₃SOSO₂]²⁻ and peaks attributed to [O₃SOSO₂]²⁻ in [N(CH₃)₄]₂O₃SOSO₂(s), with frequencies cm⁻¹ and relative intensities in brackets.

[O ₃ SOSO ₂] ²⁻		O ₃ ClOClO ₂			Assignment ^{c,d}			
Calculated (B3PW91/6-311+G(3df)) [O ₃ SOSO ₂] ^{2-*}		Observed in [N(CH ₃) ₄] ₂ O ₃ SOSO ₂ (s)		Calculated (B3PW91/6-311+G(3df)) O ₃ ClOClO ₂ [§]	Observed IR ^{a,b}		[O ₃ SOSO ₂] ²⁻	O ₃ ClOClO ₂
Raman	IR	Raman [N(CH ₃) ₄] ₂ O ₃ SOSO ₂	IR [N(CH ₃) ₄] ₂ O ₃ SOSO ₂	IR	O ₃ ClOClO ₂ Gas phase	O ₃ ClOClO ₂ Ne Matrix		
35 (1)	35 (<1)			41 (<1)				
45 (<1)	45 (<1)			57 (<1)				
132 (3)	132 (1)			115 (1)				
222 (42)	222 (13)	215 (84)		223 (17)			238.0	v(O ₂ S-O) ρ(ClOCl)
279 (9)	279 (<1)	277 (15)		254 (<1)			371.2	ρ(SO ₂) ρ(SO ₃) ρ(ClO ₃)
393 (4)	393 (18)	378 (8)		377 (18)			374.6	ρ(SO ₂) ρ(SO ₃) ρ(ClO ₂)
420 (1)	420 (<1)	458 (12)		429 (1)		486.6	486.0	δ _{as} (SO ₃) δ _s (ClO ₃)
479 (17)	479 (40)	477 (10)	476 (9)	490 (58)	544.0 (A, C)	543.6 (A, C) 540.2 (B, D)	542.5 (A, C) 539.1 (B, D)	δ _s (SO ₃) δ _r (SO ₂) δ(ClO ₂)
542 (10)	542 (1)	550 (3)	549 (5)	552 (3)		578.2	580.0	δ(SO ₃) δ(SO ₂) δ _{as} (ClO ₃)
575 (3)	575 (5)	591 (2)	590 (14)	584 (19)	579.0 (C, D)	585.5 (A, B) 582.8 (C, D)	585.9 (A, B) 583.0 (C, D)	ρ _r (SO ₃) δ _{as} (ClO ₃)

613 (16)	613 (2)	615 (3)	614 (15)	587 (7)	629.0 (A, C)	625.2 (A, C) 621.0 (B, D)	624.0 (A, C) 619.5 (B, D)	$\rho(\text{SO}_3)$ $\delta(\text{SO}_2)$ $\nu(\text{O}_2\text{S-O})$	$\nu(\text{O}_2\text{Cl-O})$
630 (8)	630 (48)	640 (3)	634 (21)	633 (46)	691.0 (B)	693.0 (A) 692.0 (B) 687.7 (C) 687.0 (D)	695.7 (A) 695.0 (B) 690.7 (C) 690.0 (D)	$\nu(\text{O}_2\text{S-O})$ $\delta(\text{SOS})$ $\delta_{\text{as}}(\text{SO}_3)$	$\nu(\text{O}_3\text{Cl-O})$
792 (27)	792 (84)	842 (7)	836 br (100)	716 (50)	1024.0 (C, D)	1026.3 (A, B) 1023.7 (C, D)	1026.0 (A, B) 1023.6 (C, D)	$\nu_s(\text{O}_3\text{S-O})$	$\nu_s(\text{ClO}_3)$
1039 (4)	1039 (53)	1033 (9)	1032 (47)	1063 (50)	1080.0 (A, C)	1082.3 (A, C) 1075.7 (B, D)	1081.5 (A, C) 1074.9 (B, D)	$\nu_s(\text{SO}_3)$ $\nu_s(\text{SO}_2)$	$\nu_s(\text{ClO}_2)$
						1087.1	1084.7	?	?
						1235.1 (C) 1233.8 (D)	1231.9 (C) 1228.5 (D)		$\nu_{\text{as}}(\text{ClO}_3)$
1096 (100)	1096 (10)	1104 (37)	1103 (23)	1136 (23)		1245.6 (D)		$\nu_s(\text{SO}_2)$ $\nu_s(\text{SO}_3)$	$\nu_{\text{as}}(\text{ClO}_2)$
1173 (47)	1173 (45)	1172 (3)	1168 (58)	1285 (75)		1249.5 (A) 1248.2 (B)	1245.9 (A) 1242.6 (B)	$\nu_{\text{as}}(\text{SO}_2)$ $\nu_{\text{as}}(\text{SO}_3)$	$\nu_{\text{as}}(\text{ClO}_3)$
1221 (52)	1221 (76)	1192 (19)	1210 br (87)	1304 (18)	1265.0 (A)	1263.1 (A) 1257.7 (C) 1251.3 (B)		$\nu_{\text{as}}(\text{SO}_3)$	$\nu_{\text{as}}(\text{ClO}_2)$
						1267.7	1261.7	?	?
1222 (12)	1222 (100)	1192 (19)	1210 br (87)	1321 (100)		1284.1 (A) 1282.6 (B) 1274.5 (C) 1269.3 (D)	1278.1 (A) 1276.1 (B) 1270.7 (C) 1263.7 (D)	$\nu_{\text{as}}(\text{SO}_3)$ $\nu_{\text{as}}(\text{SO}_2)$	$\nu_{\text{as}}(\text{ClO}_3)$

⁶ See geometry given in Figure S.6. ⁷ See geometry given in Figure S.7.

⁸ A – $\text{O}_3^{35}\text{ClO}^{35}\text{ClO}_2$, B – $\text{O}_3^{35}\text{ClO}^{37}\text{ClO}_2$, C – $\text{O}_3^{37}\text{ClO}^{35}\text{ClO}_2$, D – $\text{O}_3^{37}\text{ClO}^{37}\text{ClO}_2$

⁹ Assignments made by Wilner are based on a comparison with ClO_2F and ClO_3F .⁹ Our visual examination of the vibrations agreed with Wilner's assignments with some exceptions.

¹⁰ Assignments made using ChemCraft.

¹¹ Vibration listed first is the main contributor with secondary contribution given on the second line. Equal contribution given on same line.

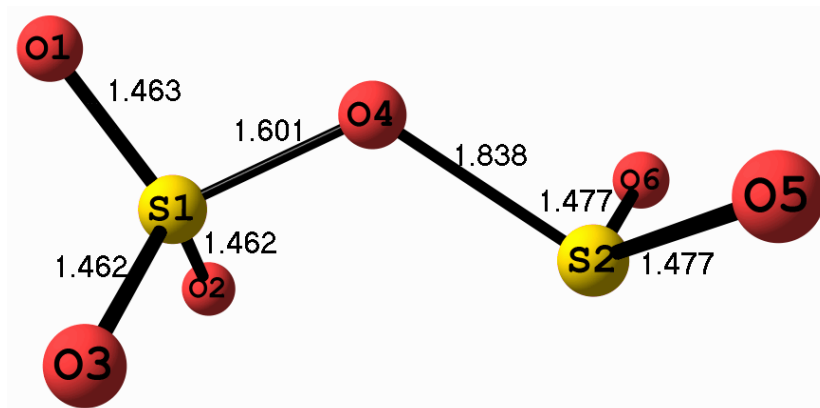


Figure S.6. Calculated (B3PW91/6-311+G(3df)) gas phase structure of $[\text{O}_3\text{SOSO}_2]^{2-}$ with bond lengths (Å).

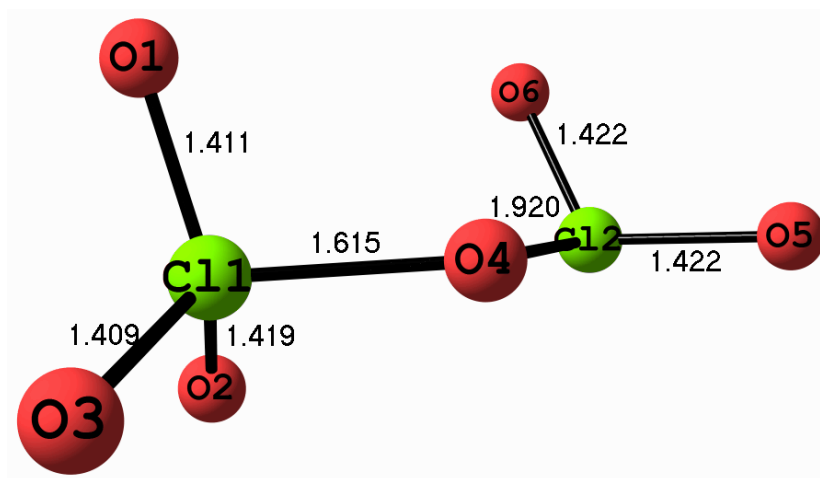


Figure S.7. Calculated (B3PW91/6-311+G(3df)) gas phase structure of Cl_2O_6 with bond lengths (Å).

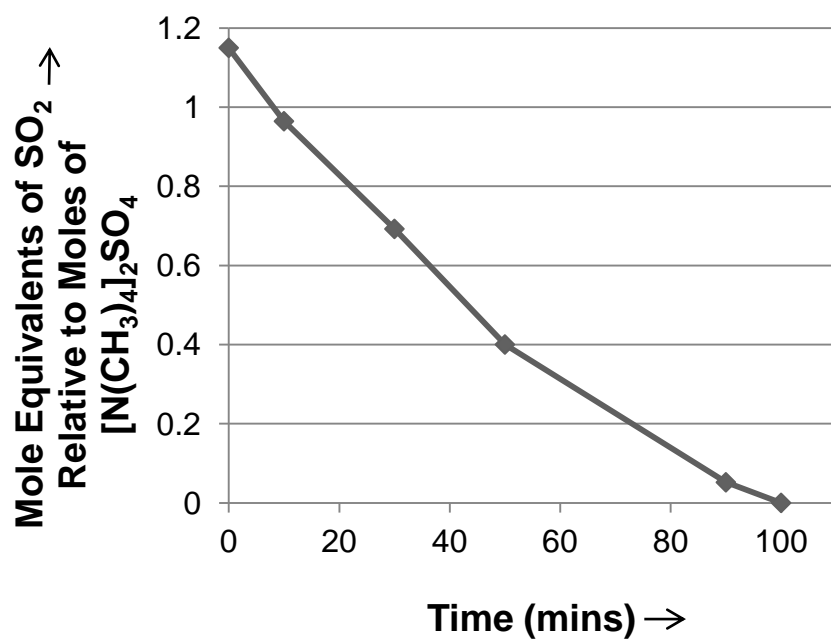


Figure S.8. Loss of SO₂ on evacuation of [N(CH₃)₄]₂O₃SOSO₂(s) as a function of time.

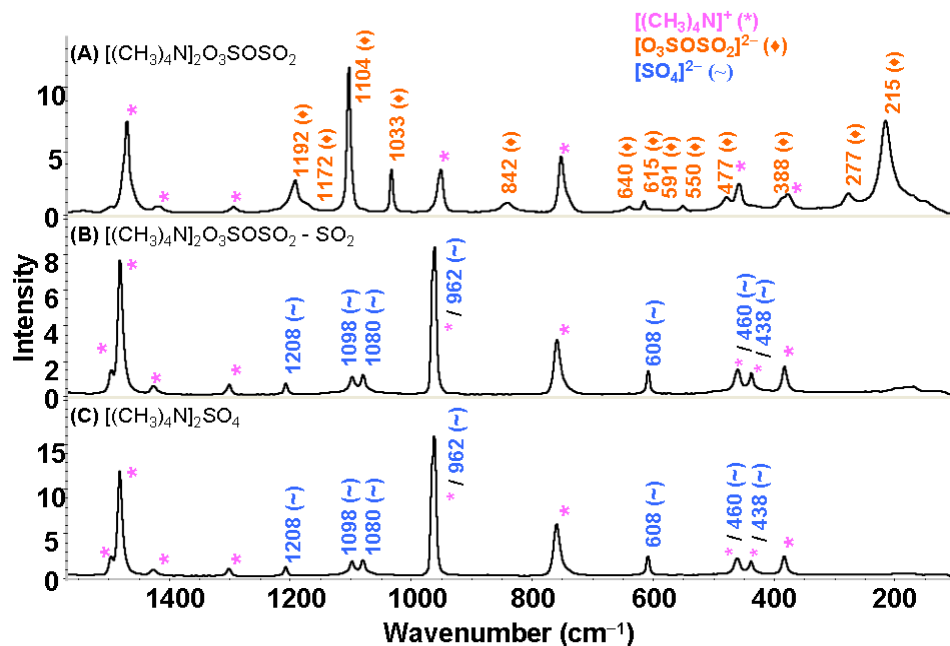


Figure S.9. Raman of $[\text{N}(\text{CH}_3)_4]_2\text{SO}_4(\text{s})$ after the removal of SO_2 (B) from $[\text{N}(\text{CH}_3)_4]_2\text{O}_3\text{SOSO}_2(\text{s})$ (A) compared with that of $[\text{N}(\text{CH}_3)_4]_2\text{SO}_4(\text{s})$ (C) in 140 - 1500 cm^{-1} region (Scans: 2048; Resolution: 4cm^{-1} ; Detector: Ge) with A and B laser power of 0.205 W and C laser power of 0.216 W.

Table S.4. Crystal data and structure refinement for [N(CH₃)₄]₂(O₂SO)₂SO₂•SO₂(s).

Compound Name	[NMe ₄] ₂ SO ₄ ²⁻ •3SO ₂
Empirical formula	C ₈ H ₂₄ N ₂ O ₁₀ S ₄
Formula weight	436.53
Temperature	173(1) K
Wavelength	0.71073 Å
Diffractometer used	Bruker AXS P4/SMART 1000
Detector distance	5 cm
Monochromator used	Graphite
Crystal size	0.60 x 0.60 x 0.40 mm ³
Colour and habit	Colourless, irregular
Crystal system	Monoclinic
Space group	P2(1)/n
Unit cell dimensions	a = 10.270(3) Å
	b = 15.265(4) Å
	c = 13.278(5) Å
	α = 90°
	β = 112.117(4)°
	γ = 90°
Volume	1928.5(10) Å ³
Z	4
Density (calculated)	1.503 Mg/m ³
Absorption coefficient	0.539 mm ⁻¹
F(000)	920
Theta range for data collection	2.13 to 27.50°
Completeness to theta = 25.00°	100.0 %
Scan type	ω and φ
Scan range	0.3°
Exposure time	10s
Index ranges	-13 ≤ h ≤ 12, -19 ≤ k ≤ 19, -16 ≤ l ≤ 12
Standard reflections	50 frames at beginning and end of data collection
Crystal stability	no decay
Reflections collected	8239
Independent reflections	4327 [R(int) = 0.0453]
Solution	Direct methods
Hydrogen atoms	Calculated positions, riding model
Absorption correction	SADABS
Max. and min. transmission	0.8132 and 0.7380
Refinement method	Full-matrix least-squares on F ²
Data / restraints / parameters	4327 / 0 / 225
Goodness-of-fit on F ²	1.042
Final R indices [I>2sigma(I)]	R1 = 0.0543, wR2 = 0.1503
R indices (all data)	R1 = 0.0776, wR2 = 0.1634
Largest/mean shift/esd	0.000/0.000
Largest diff. peak and hole	0.847 and -0.391 e.Å ⁻³

$$wR2 = (\sum[w(F_o^2 - F_c^2)^2] / \sum[wF_o^4])^{1/2}$$

$$R1 = \sum ||F_o| - |F_c|| / \sum |F_o|$$

$$\text{Weight} = 1 / [\sigma^2(F_o^2) + (0.0941 * P)^2 + (0.5498 * P)] \text{ where } P = (\max(F_o^2, 0) + 2 * F_c^2) / 3$$

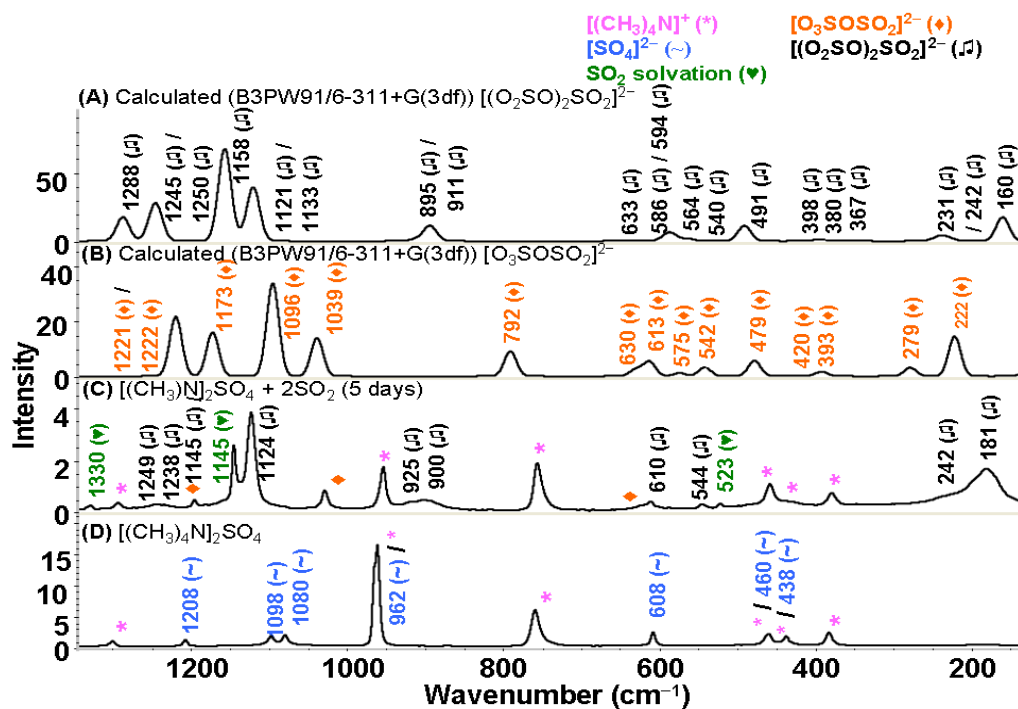


Figure S.10. Raman of $[\text{N}(\text{CH}_3)_4]_2\text{SO}_4 + 2.07 \text{SO}_2(\text{s})$ obtained after 5 days (C) compared with that of $[\text{N}(\text{CH}_3)_4]\text{SO}_4(\text{s})$ (D) and calculated spectrum of $[(\text{O}_2\text{SO})_2\text{SO}_2]^{2-}$ (A) in $160 - 1300 \text{ cm}^{-1}$ region (resolution: 4 cm^{-1}) where (C) has 1024 scans, use InGaAs detector and laser power of 0.205 W and (D) has 2048 scans, used a Ge detector and laser power of 0.216 W. (A) and (B) are calculated spectra.

Table S.5. The experimental vibrational spectrum (frequencies cm^{-1} , relative intensities in brackets) of $[(\text{O}_2\text{SO})_2\text{SO}_2]^{2-}$ in the solid obtained from the addition of 2.07 mole equivalent of SO_2 to 1 mole of $[\text{N}(\text{CH}_3)_4]_2\text{SO}_4(\text{s})$, compared with the calculated (B3PW91/6-311+G(3df)) spectrum.

$[\text{N}(\text{CH}_3)_4]_2[(\text{O}_2\text{SO})_2\text{SO}_2] \cdot \text{SO}_2(\text{s})$	Calculated [(B3PW91/6-311+G(3df)) for $[(\text{O}_2\text{SO})_2\text{SO}_2]^{2-}$	Assignment ^{a,b,c,d}
	12 (1)	A $\rho_t(\text{SO}_2)$
	13 (<1)	B $\rho_t(\text{SO}_2) + \rho_r(\text{SO}_2)$
	29 (<1)	A $\rho_r(\text{SO}_2)$
	48 (<1)	B $\rho_r(\text{SO}_4)$ $\rho_r(\text{SO}_2)$
	110 (8)	A $\delta(\text{O}_3\text{S-O-SO}_2)$
	110 (1)	B $\rho_t(\text{SO}_4)$ $\delta(\text{O}_3\text{S-O-SO}_2)$
169 sh (15)	160 (19)	A $\rho_t(\text{O}_3\text{SO-SO}_2)$
181 (98)	161 (6)	B $\nu_{\text{as}}(\text{O}_3\text{SO-SO}_2)$
	232 (4)	A $\rho_t(\text{SO}_2)$
242 sh (40)	243 (4)	B $\rho_t(\text{SO}_2)$ $\rho_r(\text{SO}_4)$
342 (<1)	367 (1)	A $\delta(\text{SO}_4)$ $\rho_w(\text{SO}_2)$
354 (<1)	381 (<1)	B $\rho_w(\text{SO}_2)$
380 (17)		Cation
432 (10)		Cation
459 (24)	398 (1)	A $\delta(\text{SO}_4)$ $\rho_w(\text{SO}_2)$ + Cation
496 (7)	492 (17)	A $(\text{O}_4\text{S}^{2-}\text{-OSO})$ $\delta(\text{SO}_2)$
523 (5)		SO_2 solvation (SOS bend)
544 (5)	541 (<1)	B $\delta(\text{SO}_2)$ $\delta(\text{SO}_4)$
564 (<1)	564 (2)	A $\delta(\text{SO}_2)$ $\delta(\text{SO}_4)$
578 (<1)	586 (8)	A $\delta(\text{SO}_4)$ $\delta(\text{SO}_2)$
593 (2)	595 (2)	B $\delta(\text{SO}_4)$ $\delta(\text{SO}_2)$
610 (5)		SO_4^{2-}
619 (7)	633 (1)	B $\delta(\text{SO}_4)$ $\delta(\text{SO}_2)$
757 (38)		$\nu_3(\text{A}_1) \nu_{\text{sym}}\text{C}_4\text{N}$ $\nu_s\text{C}_4\text{N}$
900 (19)	894 (16)	A $\nu_{\text{sym}}(\text{SO}_4)$ $\nu_{\text{sym}}(\text{SO}_2)$
925 (7)	912 (2)	B $\nu_{\text{as}}(\text{SO}_4)$ $\nu_{\text{sym}}(\text{SO}_2)$
955 (31)		$\nu_{18}(\text{F}_2)\nu_{\text{as}}\text{C}_4\text{N}$ $\nu_{\text{as}}\text{C}_4\text{N}$
1030 (6)		$\text{S}_2\text{O}_6^{2-}$

1103 sh (10)		$S_2O_6^{2-}$
1124 (100)	1121 (56)	A $\nu_{sym}(SO_2)$; $\nu_{sym}(SO_4)$
	1133 (2)	B $\nu_{sym}(SO_2)$ $\nu_{as}(SO_4)$
1145 (64)	1158 (100)	A $\nu_{sym}(SO_4)$ $\nu_{sym}(SO_2)$ + SO_2 solvation ($\nu_{sym} S-O$)
1185 (5)		$S_2O_6^{2-}$
1197 (5)		$S_2O_6^{2-}$
1238 (5)	1245 (29)	B $\nu_{as}(SO_2)$ $\nu_{as}(SO_4)$
1249 (2)	1250 (14)	A $\nu_{as}(SO_2)$ $\nu_{as}(SO_4)$
1294 (7)	1288 (26)	B $\nu_{as}(SO_4)$ $\nu_{as}(SO_2)$ $\nu_{17}(F_2)CH_3$ rock
1330 (5)		SO_2 solvation ($\nu_{asym} S-O$)
1419 (5)		$\nu_{16}(F_2)\delta_{sym}CH_3$
1465 (19)		Cation
1474 (29)		$\nu_6(E)\delta_{as}CH_3$
1501 (10)		$\nu_{15}(F_2)\delta_{as}CH_3$
2834 (19)		$\nu_{13}(F_2)\nu_{as}CH_3$
2929 (74)		$\nu_5(E)\nu_{as}CH_3$ $\nu_{14}(F_2)\nu_{sym}CH_3$
2968 (62)		$\nu_1(A_1)\nu_{sym}CH_3$ + combination bands
3034 (93)		

^a Assignments all related to $N(CH_3)_4^+$ follow that given for $N(CH_3)_4^+$ in $[N(CH_3)_4]_2SO_4(s)$.⁷

^b bands were assigned visually with the aid of ChemCraft; ν - stretching, δ - bending, ρ - twisting/rocking/wagging

^c Ten of the expected 27 vibrations were observed experimentally while eight (12 cm^{-1} (A), 13 cm^{-1} (B), 29 cm^{-1} (A), 48 cm^{-1} (B), 110 cm^{-1} (A), 110 cm^{-1} (B), 161 cm^{-1} (A), 161 cm^{-1} (B)) were too low in frequency to be observed. The remaining 9 calculated vibrations (169 cm^{-1} (B), 342 cm^{-1} (A), 354 cm^{-1} (B), 459 cm^{-1} (A), 496 cm^{-1} (A), 564 cm^{-1} (A), 578 cm^{-1} (A), 593 cm^{-1} (B), 1294 cm^{-1} (B)) had very low calculated intensities and therefore were not observed or were buried in cation or other anion bands.

^d Vibration listed first is the main contributor with secondary vibrations following.

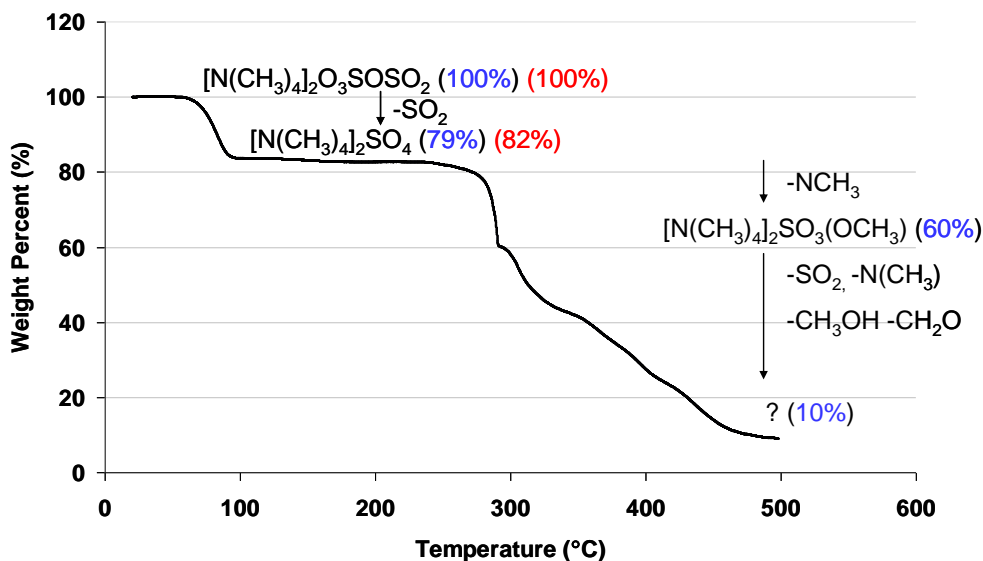


Figure S.11. TGA of $[N(CH_3)_4]_2O_3SOSO_2$. Blue numbers indicated expected weight percent and red numbers indicate experimental value.

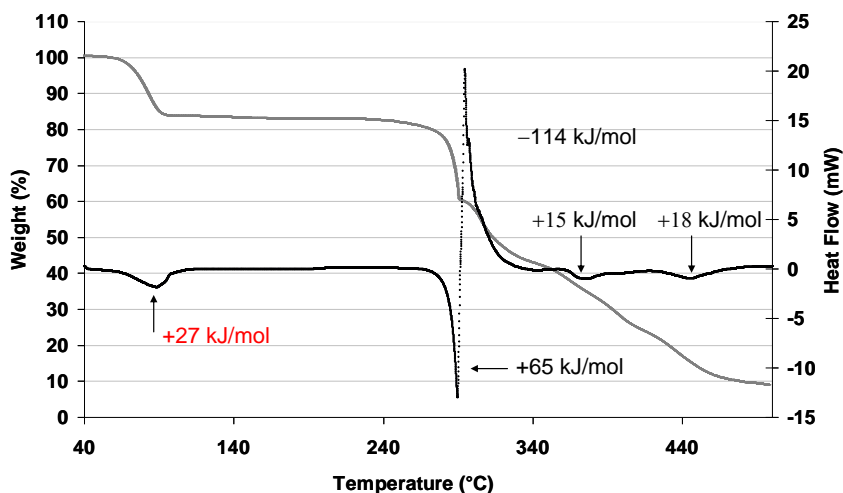
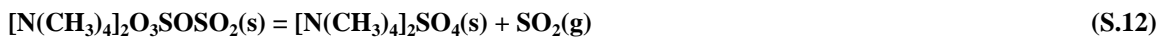


Figure S.12. DSC of $[N(CH_3)_4]_2O_3SOSO_2$. TGA outlined in grey.



The DSC (Figure S.12) gave an enthalpy of reaction S.12 as +27 kJ/mol at approximately 90 °C. This is a lower limit as there is $SO_2(g)$ loss on manipulation. A much more reliable value of the enthalpy of reaction S.11 can be obtained from a temperature dependence study of the vapour pressure of $SO_2(g)$ over $[N(CH_3)_4]_2O_3SOSO_2(s)$. We report numerical

values for the energy changes above 200 °C that correspond to decomposition of $\text{N}(\text{CH}_3)_4\text{SO}_4(\text{s})$ which are not reported in Malchus and Jansen's DTA studies.

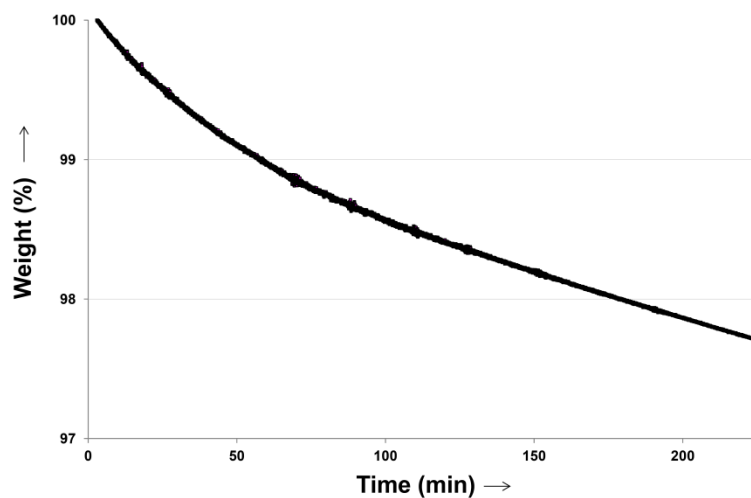


Figure S.13. TGA of $[\text{N}(\text{CH}_3)_4]_2\text{O}_3\text{SOSO}_2$ as a function of time.

Table S.6. A comparison of Av S-O bond distances (Å), OSO bond angle (°) and Raman frequency⁸ (frequencies cm^{-1} , relative intensities in brackets) in $[\text{N}(\text{CH}_3)_4]_2\text{O}_3\text{SOSO}_2 \cdot \text{SO}_2(\text{s})$, $\text{SO}_2(\text{g})$ and $\text{SO}_2(\text{s})$.

	Av S-O (Å)	O-S-O (°)	ν_s (cm^{-1})	ν_{as}	δ
$\text{SO}_2(\text{g})$ ^{i,10}	1.4343(3)	119.5(10)	1334	1150	524
$\text{SO}_2(\text{s})$ (185 K) ¹¹	1.4297(7)	117.5(1)	1341	1148	523
$[\text{N}(\text{CH}_3)_4]_2(\text{O}_2\text{SO})_2 \cdot \text{SO}_2(\text{s})$ (this work)	1.394(4) 1.344(4)	120.022(2)	1331 (5)	1145 (64)	523 (5)

ⁱ Raman vibrations are for $\text{SO}_2(\text{l})$.

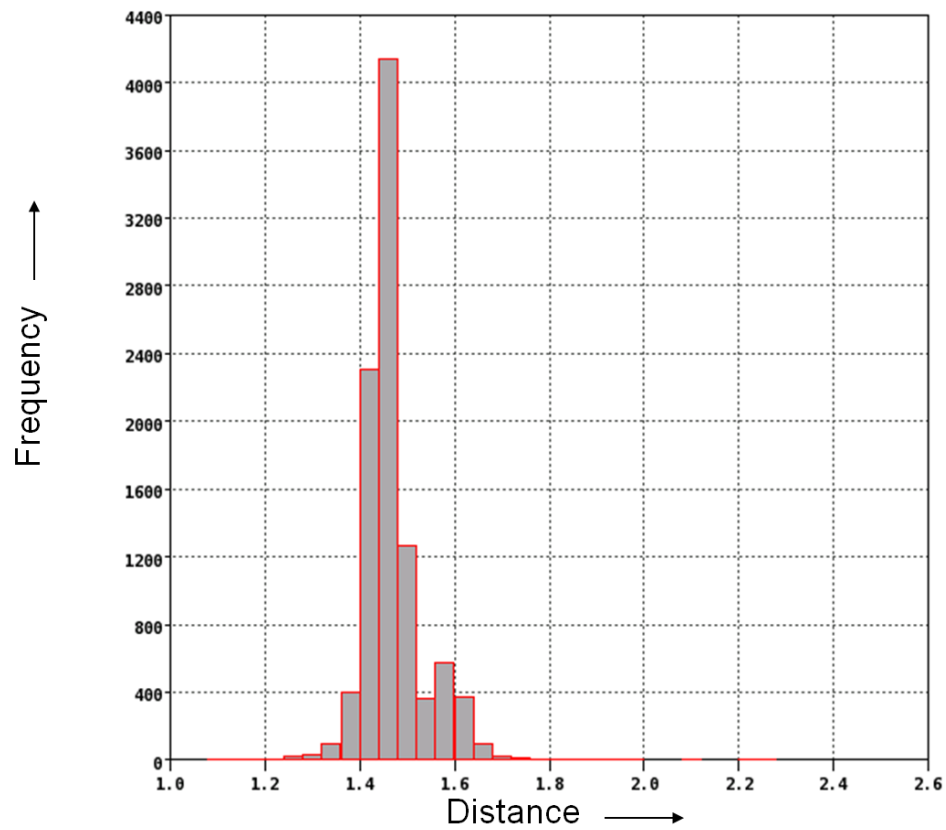


Figure S.14. Frequency of S-O bond distances from Cambridge Crystallographic Data Centre (August 2011).

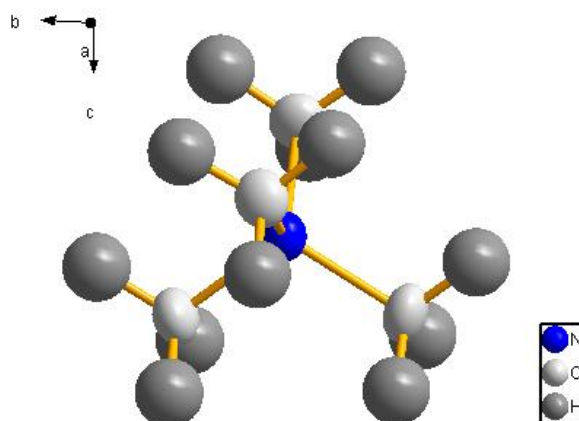


Figure S.15. Diamond depiction of $\text{N}(\text{CH}_3)_4^+$ in $[\text{N}(\text{CH}_3)_4]_2(\text{O}_2\text{SO})_2\text{SO}_2 \cdot \text{SO}_2(\text{s})$.

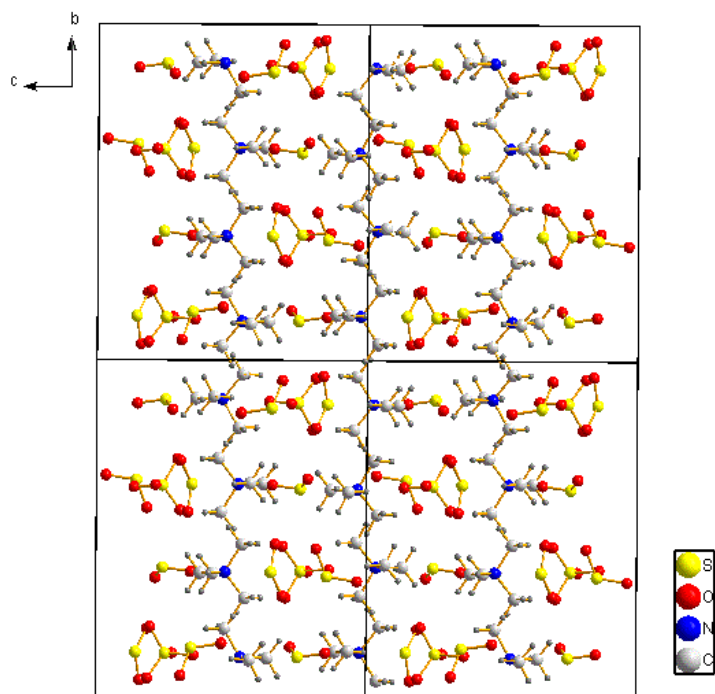


Figure S.16. Crystal packing of $[\text{N}(\text{CH}_3)_4]_2(\text{O}_2\text{SO})_2\text{SO}_2 \cdot \text{SO}_2(\text{s})$ along the a axis using $2 \times 2 \times 2$ unit cells. Hydrogen atoms were removed for clarity.

Table S.7. Cation anion contacts in $[\text{N}(\text{CH}_3)_4]_2(\text{O}_2\text{SO})_2\text{SO}_2 \cdot \text{SO}_2(\text{s})$.

No. (C-H ^a ----O)	d(H---O) (Å)	<(C-H----O) (°)
C2-H2C---O1	2.536	147.87
C1-H1A---O1	2.453	150.98
C3-H3B---O2	2.671	166.42
C2-H2A---O2	2.385	162.60
C7-H7C---O2	2.516	164.60
C4-H4C---O3	2.680	158.83
C6-H6C---O3	2.660	140.43
C8-H8B---O3	2.395	149.51
C5-H5A---O3	2.492	145.69
C5-H5C---O3	2.660	156.90
C6-H6A---O4	2.598	160.90
C4-H4A---O4	2.600	142.27
C3-H3C---O4	2.432	147.82
C1-H1C---O4	2.477	146.36
C7-H7A---O4	2.622	158.48
C7-H7B---O6	2.659	173.00
C4-H4B---O8	2.708	152.06
C2-H2B---O7	2.708	159.59

^aC-H distance fixed at 0.9800 Å

Table S.8. Comparison of the geometry of $[\text{N}(\text{CH}_3)_4]^+$ in $[\text{N}(\text{CH}_3)_4]_2(\text{O}_2\text{SO})_2\text{SO}_2 \cdot \text{SO}_2$ to other known $[\text{N}(\text{CH}_3)_4]^+$ salts.

	$[\text{N}(\text{CH}_3)_4]_2(\text{O}_2\text{SO})_2\text{SO}_2 \cdot \text{SO}_2$	$[\text{N}(\text{CH}_3)_4]_2\text{SO}_4$ (173 K) ⁷
N-C1 (Å)	1.5034(31)	1.492(3)
N-C2 (Å)	1.482(4)	1.492(3)
N-C3 (Å)	1.498(3)	1.492(3)
N-C4 (Å)	1.496(3)	1.492(3)
C1-N-C2 (°)	109.935(2)	109.2(2)
C4-N-C1 (°)	109.730(2)	109.5(3)
C2-N-C4 (°)	108.638(2)	
C3-N-C4 (°)	109.445(2)	
C3-N-C1 (°)	109.443(2)	109.6(2)
C2-N-C3 (°)	109.634(2)	109.7(3)

References

1. Jenkins, H.D.B.; Passmore, J.; Glasser, L. *Inorg. Chem.* **1999**, *38*, 3609.
2. Glasser, L.; Jenkins, H.D.B. *J. Chem. Eng. Data* **2011**, *56*, 874.
3. Bryan, J.C., Burnett, M.N., Gakh, A.A., *Acta Cryst.*, **1998**, *C54*, 1229.
4. Herbstein, F.H, Kaftory, M., Kapon, M., Saenger, W., *Z. Kristallogr. Kristallgeom. Kristallphys. Kristallchem.*, **1981**, *154*, 11.
5. Wang, Q., Habenschuss, A., Xenopoulos, A., Wunderlich, B., *Mol.Cryst.Liq.Cryst.Sci.Technol.,Sect.A*, **1995**, *264*, 115.
6. Prukala, W., Marciniak, B., Kubicki, M., *Acta Crystallogr.,Sect.E*, **2007**, 63.
7. Malchus, M.; Jansen, M. *Acta Cryst.* **1998**, *B54*, 494.
8. Anderson, A.; Savoie, R. *Canadian Journal of Chemistry* **1965**, *43*, 2271.
9. Jansen, M.; Schatte, G.; Tobias, K. M.; Willner, H., *Inorg. Chem.*, **1988**, *27*, 1703.
10. Holder, C.H.; Fink, M. *J. Chem. Phys.* **1981**, *75*, 5323.
11. Kumar, A.; McGrady, G. S.; Passmore, J.; Grein, F.; Decken, A. *Z. Anorg. Allg. Chem.* **2012**, *638*, 744 and references within.

Curriculum Vitae

Candidate's full name: Stephanie Ann Richardson

Universities attended (with dates and degrees obtained): University of New Brunswick,
2009, Bachelor of Science - Chemistry

Publications: Bruna, P.; Decken, A.; Grein, F.; Passmore, J.; Richardson, S.; Rautianinen,
M.; Whidden, T. *Inorganic Chemistry* accepted.

Bruna, P.; Decken, A.; Greer, S.; Grein, F.; Jenkins, H.D.B.; Mueller, B.; Paulose,
T.A.P.; Passmore, J.; Rautiainen, J.; Richardson, S.; Schriver, M.J. *Inorganic Chemistry*
in progress.

Conference Presentations: 2011 Poster presentation at CSC (Montreal, Quebec), 2012

2012 2nd place oral presentation at AIDW (Charlottetown,
PEI)